1-1-2007

Experimental Determination of Carbon Dioxide Diffusivity in Low-density Polyethylene

Jitendra Tendulkar
Ryerson University

EXPERIMENTAL DETERMINATION OF CARBON DIOXIDE DIFFUSIVITY IN LOW-DENSITY POLYETHYLENE

By

Jitendra Tendulkar

Bachelor of Engineering
Kolhapur University
Maharashtra, India, 1990

A thesis
presented to Ryerson University
in partial fulfillment of the
requirement for the degree of
Master of Applied Science
in
Chemical Engineering

Toronto, Ontario, Canada, 2007

Author's Declaration

I hereby declare that I am the sole author of this thesis.

I authorize Ryerson University to lend this thesis to other institutions or individuals for the purpose of scholarly research.

Jitendra Tendulkar

I further authorize Ryerson University to produce this thesis by photocopying or by other means, in total or part, at the request of other institutions or individuals for the purpose of scholarly research.

Jitendra Tendulkar

Abstract

EXPERIMENTAL DETERMINATION OF CARBON DIOXIDE DIFFUSIVITY IN LOW-DENSITY POLYETHYLENE

Jitendra Tendulkar

Master of Applied Science, 2007

Department of Chemical Engineering

Ryerson University

Diffusion in molten polymers far above the glass-transition temperature is characteristic of many industrial processes such as polymerization, monomer recycling, stripping, drying, coating and foaming. Many of these systems of practical importance exhibit a strong dependence of diffusion coefficients on concentration and temperature. These operations involve concentrated solutions of polymers and solvents, which are far removed from the dilute region where theoretical advancements have been most significant. The design and optimization of these applications requires concentration dependent diffusivity data, which are scarce at present.

In this work, the calculus of variation is used to establish the necessary conditions of the concentration-dependent diffusivity for a unidirectional distributed parameter model, such that the model-predicted mass of absorbed gas in polymer matches with its

experimental counterpart. A computational algorithm is implemented to solve the model, and obtain the diffusivities of carbon dioxide gas in low-density polyethylene (LDPE) melt, in the range of 352 to 1232 kPa, at 120°C and 130°C. The optimal diffusivities versus concentration curves obtained indicate diffusivity as a significant function of concentration in the polymer medium. The peak diffusivity of carbon dioxide in low-density polyethylene melts for the above temperature and pressure range varies between $3.04\times10^{-9}\,m^2/s$ to $4.56\times10^{-9}\,m^2/s$. The above results obtained are evaluated for their sensitivity with respect to maximum expected experimental variation in saturation weight fraction of the gas. The sensitivity of diffusivity to change in above system parameters is maximum at its peak value and is less than 2% with respect to its base value.

Acknowledgment

I would like to convey my sincere thanks to everyone who helped, support and encourage me throughout this study in every way possible.

My special thanks go to Dr. Simant R. Upreti for giving me an opportunity to work on this project and also for his excellent guidance along with inspiration throughout the thesis work. From his instruction, I developed an understanding to arts and skills of a researcher and an approach to learning.

I thank Dr. Ali Lohi for his support with meaningful discussions, and guidance in developing an understanding of experimentation.

I would also like to thank Dr. Stephan Drappel, Xerox Research Centre of Canada and Dr. Joo Teh, Nova Chemicals for their help in characterization of the polymer sample.

I appreciate the indisputable support that I received from the mechanical workshop team Mr. Peter Scharping and Mr. Ali Hemmati during the lab setup. I also appreciate the support I received from the electrical lab supervisor; Mr. Tondar Tajrobehkar. Without their support it would not be possible for me to complete this experimental research.

I also would like to thank Canada Foundation of Innovation; Ontario Innovation Trust; Natural Sciences and Engineering Research Council (NSERC) of Canada; and Department of Chemical Engineering, Ryerson University; for funding the activities in the project.

Table of Contents

List of Tables

List of Figures

Nomenclature

d	internal diameter of the pressure vessel, m
D	Fick's diffusivity of gas in LDPE, $m^2 s^{-1}$
I	objective functional
J	variational derivative of K
K	augmented objective functional
L	thickness of the LDPE sample, m
m_p	mass of LDPE, kg
m_g	mass of gas in the gas phase, kg
$m_{gp,m}$	calculated mass of gas absorbed in the LDPE layer, kg
$m_{gp,e}$	experimental mass of gas absorbed in the LDPE layer, kg
M_g	molar mass of gas, kg $kmol^{-1}$
P	pressure
P_i	initial pressure
P_f	final pressure
R	universal gas constant, 8314 j $kmol^{-1}$ k^{-1}
t	time, second
T	total experimental run time, second
V_T	total volume of the pressure cell, $22.4\times10^{-6} m^3$
$V_g(t)$	volume of the gas phase in the pressure cell, m^3
z	depth in the polymer layer, m

Greek Symbols

ρ_p density of polymer sample, kg m^3

ρ_{mix} density of polymer-gas, kg m^3

Γ thermodynamic non ideality factor

τ sample time

λ adjoint variable;

ω calculated gas mass fraction in LDPE

ω_{exp} experimental gas mass fraction absorbed in LDPE

ω_{sat} saturated gas mass fraction in LDPE

1 Introduction

1.1 Diffusion in polymers

From their inception as materials, it has been recognized that polymers have unique properties associated with their resistance to molecular penetration by other materials. This property led to many early applications in the coatings and film industry. It was natural that these applications further led to the study of diffusion in finished polymer products and their permeation properties. Consequently, the preponderance of diffusion studies in polymer systems have focused on the properties of solid polymers at temperatures and concentrations, which reflect the conditions during the end use applications. Now a large database exists, for diffusion in glassy polymers and elastomers near ambient conditions.

A second impetus for the study of molecular diffusion in polymer systems has been to use the molecular diffusion of small molecules in polymers as a molecular probe to elucidate molecular motion in macromolecular systems and morphology. Moreover, diffusion in dilute polymer solutions has gained importance due to its applications for advancement in the theoretical, experimental and analytical field. e.g. light scattering techniques have developed to permit detailed examinations of the rotational and transnational diffusion of macromolecules in solutions. In the infinitely dilute limit, the polymer molecules are widely dispersed and the individual chains do not interact. Consequently, statistical mechanical techniques can be applied to an ensemble of individual polymer chains in a continuum of the solvent.

Considerable effort that has been concerned with the study of diffusion in polymer systems has been directed to elucidating polymer diffusion in dilute solutions and relatively less towards the phenomena that are significant in the production and processing of polymers. In case of production and processing of polymers, efforts are more focused towards studying the properties associated with heat and momentum transfer, as these are the final control elements of any polymer-processing unit. In the

past few decades, molecular diffusion in particular has been used more and more to establish finer control on the polymer processing unit operations. Presence of diffusion in molten polymers far above the glass-transition temperature is discussed in brief in the following sections.

1.2 The role of molecular diffusion in polymer processing

The diffusion of solvents, monomers, additives, and other relatively small molecules is critical in many polymer formation and processing operations. In the formation and processing of small non-polymeric molecules, mixing or some other modification of the fluid mechanics can accelerate the rate of processes. Consequently, in many cases, fluid mechanical considerations are of primary importance and the diffusion coefficients involved are secondary. However, the very high viscosities, which are characteristic of polymer systems often, eliminate the practicality of significantly enhancing mass transfer by modifications of the fluid mechanics. Under these conditions, a diffusion coefficient can often be the dominant physical property in process analysis.

1.3 Diffusion and polymer reactions

Mass transfer is perhaps most prominent in the initial formation of polymers. In many cases, the rate at which a polymerization reaction proceeds is controlled or strongly influenced by the molecular diffusion of monomers, initiators, long-chain radicals, dead polymer chains, or low molecular weight condensation products. In many step polymerization reactors, the removal of condensation products can influence the rate of polymerization. For reversible reactions, the condensation by-product must be removed in order to drive the polymerization reaction toward completion. For example, in the glycol condensation route for producing polyethylene terephthalate, the diffusion of the eliminated glycol molecule from the melt can control the rate of polymerization and the properties of the produced polymer. In idealized kinetic studies of polymerization reactions, diffusion effects can often be neglected. However, these effects become

particularly important in the analysis of commercial polymerization reactors where sharp gradients in concentration often occur. In case of bulk polymerization reactors with high yields per reactor volume, the importance of mass transfer and reactor design becomes more prominent. For example, an ideal reactor for the production of a polymer by free-radical chain kinetics would be a continuous tubular flow reactor. In principle, monomer and initiator flows in from one end and a high concentration of polymer are produced at the outlet. Such a reactor involves a complex coupling of fluid mechanics, polymerization kinetics, heat transfer, and molecular diffusion.

At the high conversions, which are desirable, the main problem is the buildup of polymer concentration near the tube walls, which ultimately leads to "plugging". This phenomenon could be possibly eliminated by a high diffusion rate of the monomer into this high polymer concentration region and correspondingly a high diffusion rate of the polymer into the monomer rich center of the tube. The modeling of this radial diffusion can play a critical role in the evaluation of such reactors. Even the use of catalysis for polymer formation by chain polymerization kinetics does not eliminate the importance of monomer diffusion. Brockmeier and Rogan[1] have shown that the diffusion of monomer through a growing polymer shell around the catalyst can significantly influence the overall rate of polymerization in a polypropylene slurry reactor. An extreme low conversion reactor means high-energy consumption reactors, which would almost mean production of a non-sellable polymer.

On the other hand for high conversion reactors, it is well known that the conventional low conversion free radical kinetics does not apply over the entire conversion range in concentrated polymerization systems. At higher conversions, the steps later to propagation in case of high conversion reactors are significantly dominated by molecular diffusion controlled mass transfer in a medium similar to polymer melts. Monomer molecules and long chain radicals compete for each available free radical. When two long chain radicals come together by molecular diffusion, termination occurs. At high conversions, the decrease in the molecular diffusion of the long chain radicals cause a rapid increase in the rate of polymerization, which is termed the auto acceleration or Trommsdorff-Norrish effect. This phenomenon is due to the difference in the

concentration dependence of the diffusivities of the two competing species. Mass transfer in most polymer formation and processing operations involves the mutual diffusion of the polymer with a relatively low molecular weight species such as the monomers. The region near Trommsdorff-Norrish effect involves also the self-diffusion of long chain free radicals.

1.4 Diffusion and devolatilization

Several applications such as condensation polymerization, monomer recycle, stripping, drying, coating and foaming can be grouped under a category which involves devolatilization in its one or the other form. Devolatilization or the reverse is comprised of diffusion through the condensed phase toward the interface, phase change and diffusion into the gas phase. Molecules of volatile substance traveling into or from the condensed phase participate in these processes in series. The rate, amount and pattern of the removal of volatile components from polymer impart important physical and chemical properties to the polymer products.

One of the crucial tasks of the polymer products used in food handling is the removal of small amounts of volatile residuals to meet environmental, health, and safety regulations. In the early days of the industry, polymer devolatilization was employed to recover the monomer and to control the properties of the polymers. Consequently, it was not particularly critical to attain very low concentrations of monomer or other volatile residuals. However, over last couple of decades the focus has gradually shifted or rather widened over the ongoing concern with the potentially carcinogenic nature of some materials present within the polymer matrix. This concern has placed an emphasis on reducing residual volatile concentrations to extremely low values. This reduction is particularly difficult since the mutual binary diffusion coefficient often decreases drastically at low solvent concentrations.

In order to overcome this difficulty mechanical mixing coupled with molecular diffusion is used to design multistage processes for removal of volatiles.[2] e.g. Vacuum or steam

stripping are used in many different types of equipment such as wiped film evaporators and vented extruders to remove volatile residuals from polymer melts. Biesenberger[3] has shown that the success of such process modeling depends on the availability of information concerning the concentration and temperature dependency of diffusion coefficients in polymer melts. Another aspect of solute adsorption in polymer is morphology, which in turn can be the function of melt diffusion at the earlier production stages in the process.

1.5 Diffusion and morphology

The porosity and other morphological characteristics of the polymer particle are fixed during the polymerization process, which involves coupling of a chemical reaction, molecular diffusion, and phase equilibrium. This diffusion controlled structure then influences the desorption of monomer coming out of the melt in gaseous form during devolatilization and also the subsequent diffusion of plasticizers into the melt. The control of polymer morphology by diffusion of gases into melts during polymerization and polymer crystallization is a potentially powerful technique. The production of porous PVC particles and porous ion exchange resins are two examples of this technique.

Diffusion can be used to control the morphology of a polymer, independent of the polymerization process. Crystallization of polymers under nitrogen or carbon dioxide pressure to improve polymer micro-void structure is one of the examples.

1.6 Motivation of diffusion measurement in melts

The previous section showed that molecular diffusion influences nearly all phases of polymer formation and processing, to a measurable extent; and concurrently, process operations influence the diffusion characteristics of the final polymer product. It can also be seen that most of these processing operations occur in the melt temperature range. One of the reasons for this fact could be that, polymer melt is the phase where the polymer

mass actually comes very close to the assumption of local equilibrium. What ever we do to it at this stage gets uniformly distributed and what ever we measure of it represents the bulk to the closest estimate. Under these conditions, the polymer is in a defined equilibrium liquid state and also relatively closer to the final process output as compared to dilute solutions. A basic understanding of diffusion behavior in this relatively idealized state, should lead to progress in other more complex areas.

Because of the above reason, it could be argued that concentration dependent diffusion in polymer melts above melt temperatures is a natural starting place for the study of diffusion in polymer processes similar to devolatilization, crystallization, foaming. Though the first step in the analysis of processes involving molecular diffusion would be the measurement of the necessary diffusion coefficients, it would also be appropriate to simultaneously consider methods of generating relevant experimental data. Proper mode of data generation if employed will generate results more suitable for use in process. In this project, devolatilization is the process of interest.

2 Literature

Objective: An overview of Fick's diffusivity as a temperature and concentration dependent function in the medium and an introduction to permeation and sorption experiments, which are the two most frequently, used indirect modes of generating experimental data for diffusivity calculations.

2.1 Diffusivity in polymer melts – gas system

Diffusivity as a transport property can be defined as a ratio of medium-relative mass flux of a species to the negative of its concentration gradient along the flux. Diffusion coefficients in conventional liquid systems composed of relatively low molecular weight molecules usually fall in the magnitude range of $10^{-5}\mathrm{cm}^2/\mathrm{s}$ under ambient conditions, and also are in the most cases very weak functions of temperature and concentration. But under similar conditions large variation in diffusivity behavior is observed when one of the chemical species is a polymer. The diffusion coefficients for polymer – solvent systems can be very strong functions of state of the polymer as well as temperature and concentration. Fick's diffusivity D is related to the true transport property called Maxwell-Stefan diffusivity,[4] $\mathcal{D}$ as follows

$$D = \mathcal{D}\frac{\partial \ln a}{\partial \ln x} \equiv \mathcal{D}\Gamma \tag{2.1}$$

In the above expression: a is the activity of the species; x is it's mole fraction in the medium and Γ is the thermodynamic non-ideality factor related to concentration. Above expression indicates that (Fick's) diffusivity should not be expected to be constant at a given temperature and pressure. Depending upon the non-ideality, diffusivity of a species may vary with its concentration in the medium, and with the effect being significant for low solvent concentrations, and for larger size solvent molecules.

2.1.1 Temperature dependence

The temperature dependency of mutual binary diffusion coefficient for solvents in polymer melts does not usually follow a conventional type of relationship with activation energy. In conventional type activation energy relation, the graph of logarithm of diffusivity versus reciprocal of absolute temperature yields a straight line whose slope is

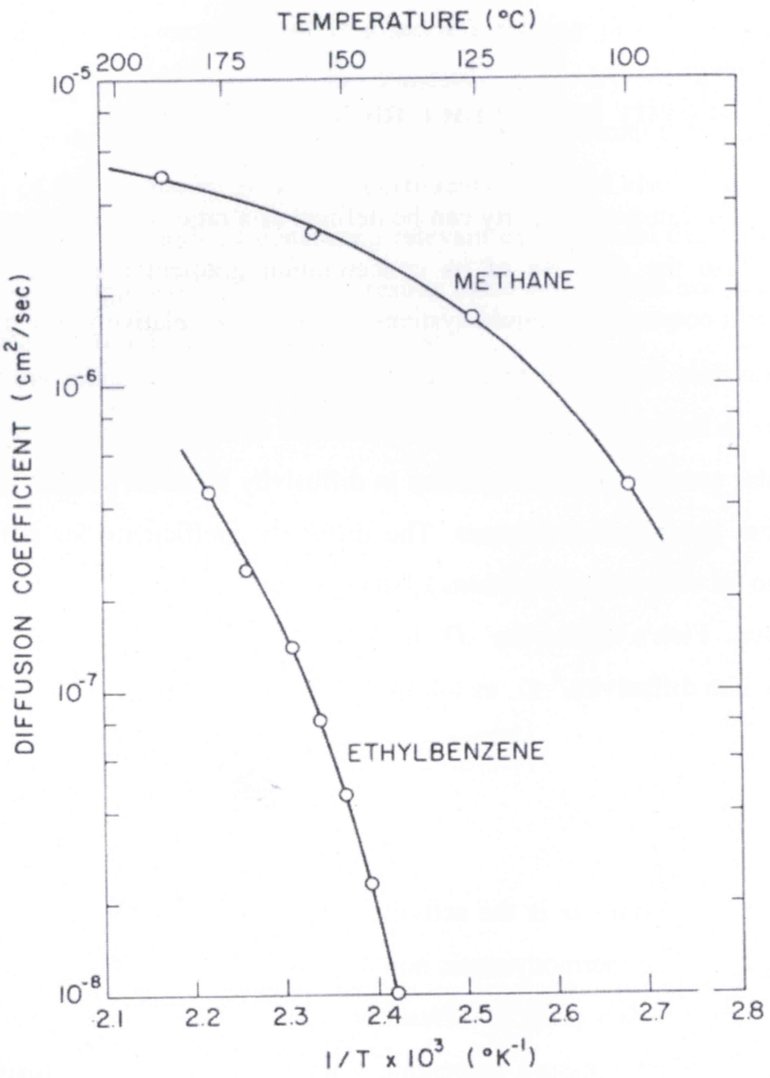

Figure 2. 1: Diffusivity versus Temperature for methane-polystyrene and ethyl benzene-polystyrene.[3]

related to the activation energy from the diffusion process. As Figure [2.1][3] indicates the apparent activation energy for polymer system can be a strong function of temperature, and large errors can occur in data generation through extrapolation. In most of the polymer – solvent systems the apparent activation energy will be larger at the lower temperature and will be smaller for the lower molecular weight solvent. For very small molecules such as fixed gases and water, the activation energy will be small thus making the diffusivity, a weak function of temperature.

2.1.2 Concentration dependence

Figure [2.2][3] shows the concentration dependent diffusion coefficient of ethyl benzene in molten polystyrene. As this figure indicates, a very small amount of solvent can cause a very large increase in the diffusion coefficient. This behavior is particularly prominent at low solvent concentration and also at the temperatures near T_g. In most cases, the variation of diffusivity with solvent concentration is decreased as the size of the solvent molecule decreases. It can be concluded that rather than being an averaged single point value, diffusivity has a behavior dependent more or less on concentration. The concentration dependent diffusivity elucidates the behavior of a polymer in absorption and desorption processes and also has its bearing on the relation between solute concentration at a distance in the polymer medium. Concentration dependent diffusivity plots are irreplaceable in the production and processing of polymers, which exhibit extreme concentration dependence. In spite of the theoretical as well as practical significance, the drive for solutions based on concentration dependent diffusivities is relatively less. The reason being that mathematical solution for a model with diffusivity and concentration interdependent is computationally a tedious task. In this project a suitable indirect mode of generating experimental data, in combination with a mass transfer model is used to arrive on an expression for concentration dependent diffusivity. The expression is further solved through optimality criterion so as to match the gas mass absorbed by model with that by the experiment.

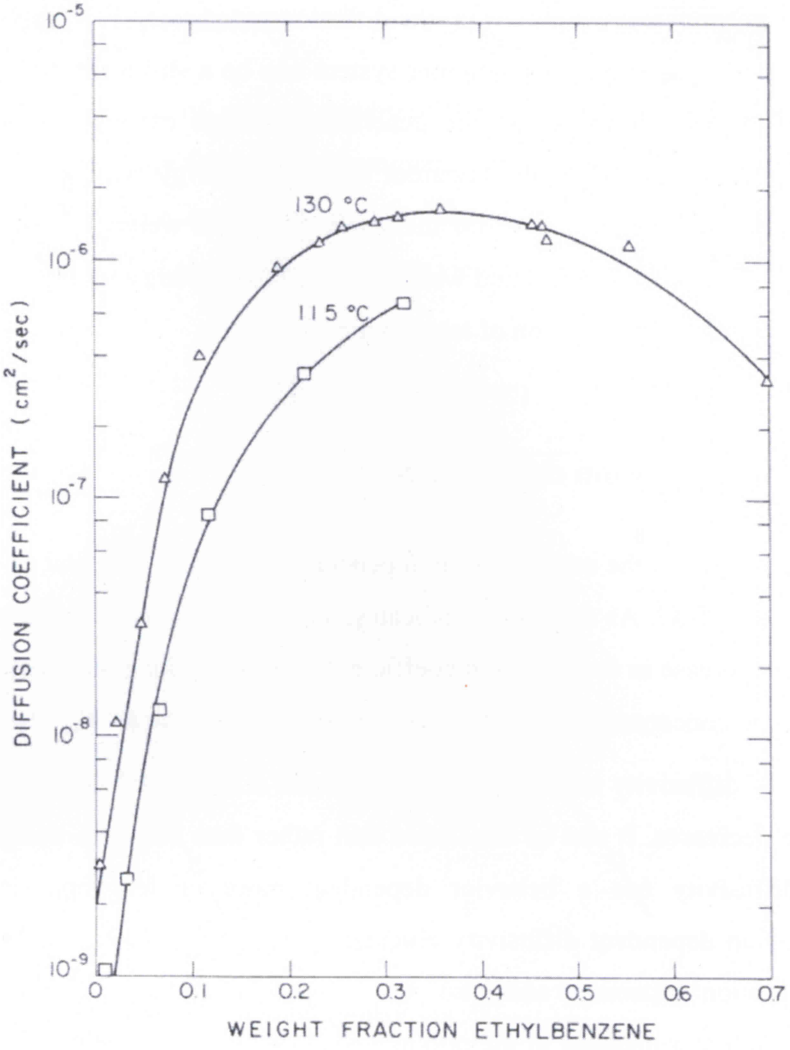

Figure 2. 2: Concentration dependent diffusivity for the ethyl benzene-polystyrene system.[3]

2.2 Modes of measurement of diffusion coefficients

There are various direct, indirect and specialized modes of generating experimental data for diffusivity calculations. To sum up, all these methods share a common goal of generating an experimental data about a parameter like sample composition, pressure, weight or volume which gives indication of the rate of mass transfer of solute into the polymer medium and also the total weight of solute mass transferable to the polymer. Each method has its applications and suitability. Indirect methods are non-intrusive and

so were thought to be more suitable for the purpose of measuring diffusion coefficients in polymer melts.

Permeation and sorption experiments are the two most frequently used methods for experimental determination of diffusion coefficients applicable in various devolatilization processes in polymer industry.

The permeation experiment utilizes the principle of steady state mass flow to measure the amount of permeant flowing through a thin membrane, while the sorption experiment utilizes transient mass flow to measure the mass uptake of the polymer sample due to solution formation with the sample. The diffusivity is derived by solving Fick's first and second laws of diffusion utilizing the measurements from the permeation and sorption experiments respectively.

The two methods of experimentation differ in ability of the experiment to determine the solubility of the permeant in the polymer. The permeation experiment relies on a mathematical relationship to determine the equilibrium solubility of the permeant in the polymer indirectly when steady state flow has been attained, whereas the sorption method, because it measures the mass gain of the polymer, determines the equilibrium solubility directly. Extensive research has been performed to determine the diffusivity and solubility utilizing permeation and sorption experimental techniques and a good historical perspective has been provided.[5,6] The following sections will briefly discuss some indirect diffusivity measurement by permeation and sorption method.

2.3 Permeation experiments

A permeation experiment measures the cumulative mass of the permeant that permeates through a thin membrane into a closed chamber (permeation rate measurement). Permeation is a three-step process of, dissolution at the high-pressure gas/polymer interface, diffusion of the solute through the polymer matrix, and evaporation at the low pressure polymer/gas interface on the other side of the membrane. The experiment

consists of two chambers separated by a thin membrane with the upstream permeant maintained at a constant pressure, and the downstream pressure although measurable is considered negligible compared to the upstream pressure. The pressure, or concentration, gradient created across the membrane is the driving force, which causes the permeant to flow through the membrane and into the downstream volume. Fick's first law of diffusion represents the mass flow relationship.

2.3.1 Classification of permeation experiments

Barometric, volumetric, and gravimetric techniques are three examples of permeation experiments. The barometric technique measures the permeation in membrane from the upstream volume.[7] The rate of change in the pressure of the downstream volume is utilized to calculate both the diffusivity and the permeability for pure gases, condensable vapours, and gas-vapour mixtures.[8] Many modifications and permutations of the cell have been developed.[9] The barometric method has been used for gas permeation through membranes at pressure up to 2 MPa for the calculation of diffusivity, but due to the inaccuracy involved in measuring the solubility in non-ideal situations, a sorption experiment has been used in combination to determine the equilibrium solubility.[10–12]

The volumetric technique measures the displacement of a fluid slug by the permeating gas in a capillary tube connected to the downstream volume.[13] The method is typically simpler to implement than the barometric approach, but is less sensitive to slow permeation rates and therefore is not utilized for high accuracy time-lag methods.[14] The gravimetric technique measures the weight increase in the collecting volume or the weight loss in the source volume container. The cell operates at atmospheric pressure and it is suitable for measuring high steady state permeation rates because large mass changes are easily measured.

Critique of permeation method: All three permeation methods operate at low pressures with the upper most limit of operating pressure achieved with the barometric technique. The pressure limitation is due to the method of measurement through a thin membrane, which could rupture at higher operating pressures. Also the basic calculations require the assumption of average diffusivity along with the steady state response of the membrane. Transient phase with wide concentration range as well as variation in pressures are the characteristics of devolatilization processes. Therefore, the permeation method is less suitable for measurement of concentration dependent diffusivities.

2.4 Sorption experiments

Sorption is the process of the dispersal of penetrating molecules into the polymer to form a mixture. A sorption experiment determines the cumulative mass gain of the penetrating molecules as a function of time, commonly referred to as the mass uptake relationship. With the mass uptake relationship, both the solubility and diffusivity are determined independently from the results of a single experiment.

Ideally, the polymer sample is placed in a constant pressure and temperature permeant environment, and the mass gain of the polymer is measured as a function of time. The driving force for the mass gain is the concentration gradient, which exists across the depth of the sample. The permeant will continue to diffuse into the polymer until an equilibrium solubility of the permeant is attained in the polymer.

A typical sorption experiment estimates the diffusivity, D, utilizing a one dimensional diffusion model, such as a plane sheet or a cylindrical rod. The one dimensional diffusion coefficient is determined by solving Fick's second law of diffusion. Also the solubility isotherm is determined, independent of D. The advantage of sorption method is that, the discrepancies from ideal sorption behavior will not be hidden by the results of the permeation experiment.[15] Sorption experimental methods for diffusivity measurement can be divided into three main categories as gravimetric, pressure decay, and volume decay techniques.

2.4.1 Gravimetric technique

The gravimetric technique measures the mass gain of the polymer as a function of time directly, while the pressure and volume decay techniques measure the mass gain of the polymer indirectly by monitoring the pressure change and the volume change under constant volume and constant pressure conditions, respectively.

Critique of gravimetric technique: The cumulative mass measurement of the sorption sample is achieved by various techniques. Periodic removal of the sample for weighing is one of the method used only in case of liquids as solutes and at atmospheric conditions. e.g. water in poly (methyl methacrylate),[16] cyclohexane in polystyrene,[17] and water diffusion in various polymers.[18] The continuous interruption and handling of the sample can provide serious errors in the calculated diffusivity values. For applications of sub-atmospheric pressures above difficulty is resolved by using a quartz spring measuring system referred to as McBain Balance.[19] This quartz spring method provides a means of overcoming the constant removal of the polymer sample but is limited to low operating pressures. McBain-Bakr sorption balance overcomes this limitation of sub atmospheric pressures. After the invention of McBain balance, various equipments based on the microbalance principle were developed and used as per their suitability of the applications.

Another mode of experiment is exposing several exactly identical samples in identical chambers (which is a limitation) for different time periods, until the last sample reaches equilibrium solubility. Once the equilibrium time has been determined, additional experiments must be performed prior to the equilibrium time in order to compile the mass uptake curve. Therefore, the procedure requires a large number of experiments in order to formulate a single pressure and temperature mass uptake curve. Inherently, the variation in sample characteristics, the measurement of individual sample thickness and sample preparation can contribute to significant scatter in the formulation of the mass uptake curve and the determination of diffusivity.

2.4.2 Volume decay sorption technique

The volume decay sorption technique measures the volume change of the permeant due to polymer sorption in closed system of constant pressure and temperature. Therefore, the mass uptake of the polymer is determined indirectly by measuring the volume decay of the fixed pressure system. The diffusivity is determined by solving the diffusivity differential equation in terms of the change in system volume as a function of time and the solubility is determined from the overall volume change of the experiment and the initial mass of the sample. Because the experiment is performed at constant pressure, the surface concentration of the polymer is maintained constant for the duration of the sorption experiment and the diffusion differential equation initial boundary conditions are satisfied.

Rosen[20] utilized a volume decay sorption apparatus to measure the solubility and diffusivity of acetone in cellulose acetate, methylene chloride vapour in polystyrene, and water vapour in neoprene. All measurements were performed at sub-atmospheric pressures. The system was designed as an alternative to the quartz spring apparatus and by incorporating a means to measure the volume change of the closed system as a function of time the device was able to continuously measure mass gain of the polymer in-situ. This method is used under different modifications and capabilities to measure diffusivity of solutes in polymers.

Critique of volume decay method: The volume decay method and also the pressure decay method, described later in this section are the commonly used techniques and are among the more affordable, less complicated, non-intrusive and continuous sorption techniques.[21]

In spite of the above attributes constant pressure or pressure decay, either of the above methods is preferred to the others, depending upon the utility of the data generated, type of model boundary conditions viable, type of diffusant-polymer systems, characteristics of the process, operating conditions, economic and technical need of the data generated etc.

The complexity of a constant pressure system is much greater than that of a constant volume or pressure decay system. The constant pressure system requires both the control and measurement of temperature and pressure of both the diffusant as well as the pressure cell, which means more synchronization and instrumentation. In the constant volume system once pressure decay starts the measurement of pressure and only the control of temperature around the cell is required.

2.4.3 Pressure decay sorption technique

The pressure decay method measures the pressure drop due to polymer mass gain in a closed system of known gas volume at a constant temperature. Newitt and Weale[22] first developed the pressure decay technique in 1948. This technique was used to study the solubilities of gases in polystyrene. This technique was later extended to make diffusion measurements by Lundberg et.al[23] in 1963. It was also used extensively to study the sorption of gases in glassy polymers to validate the dual mode sorption theory. During late 1970s this technique was utilized to develop various pressure decay systems to generate diffusivity data to suit the process requirements. Koros and Paul[24] developed the dual chamber method for pressure decay experiments. This experimental setup greatly improved the versatility, accuracy and the reliability of pressure decay experiments. With the measurement of the apparatus volume and recording the pressure and temperature, the mass of the permeant in the closed system is determined as a function of time. The diffusivity is determined by solving Fick's second law in terms of system pressure. Solubility is determined from the overall experiment pressure change.

Apart from the above techniques there are various other techniques as Nuclear magnetic resonance, dynamic light scattering, Gouy interferometer, Rayleigh or Mach-Zehnder interferometer, capillary method, spinning disc, wedge interferometer and other steady state methods. These methods are very subjective in applications.[25]

Transient stage diffusion is the characteristic of devolatilization processes as well as the pressure decay method; low solubility of CO_2 gas in low-density polyethylene melt; and no rotating or vibrating equipment in the experimental apparatus, which eliminates the

chances of errors due to diffusion by bulk motion. Due to the above stated reasons, pressure decay with conditioned gas was considered to be more suitable method for experimental data generation. The pressure decay mode with unidirectional molecular diffusion model would be used to derive the expression for optimum diffusivity dependent on concentration. The results obtained from the model would be checked for the sensitivity of the solution to variation in various parameters.

The diffusivity data generated by above methodology can be used in processed operations as surface treatment of polymer sheet, crystallization of polymers under gas pressures for micro void structures, and devolatilization of polymers.

3 Experimentation

For fulfillment of the objective of determining the concentration dependent diffusivity of carbon dioxide gas in LDPE melt, it was essential to determine various parameters of the isothermal pressure decay system. The data generated through experimentation will be used later to develop the function for concentration dependent diffusivity.

3.1 Pressure decay system

The experimental set up for the pressure decay system was built to support a general perspective of generating pressure decay data through experimentation with different gases and polymer melts up to temperatures of 250°C and pressures of 2750 kPa maximum. The experimental set up comprised: a sensor for tracing the movement of gas–polymer interface; pressure cell built for pressure decay experiments would be with a glass window providing complete view of the sample; pressure transmitter for measurement of pressure decay; isothermal environment for the pressure decay setup.

3.1.1 Guideline for building pressure decay system

Some of the guidelines required to be followed, while building the pressure decay system were as follows:

- Sample view: Clear unobstructed view of the melt sample inside the pressure decay cell.
- Minimum pressure gradient: The resolution of the pressure sensor would have to be higher than the minimum pressure gradient over the required sampling time, thus facilitating more precise plotting representing a ΔP.

- Diameter of the sample: The diameter of the sample is one of the factors that determine the minimum pressure gradient with respect to sampling time. Larger the minimum pressure gradient, lesser would be the accuracy of the solution, if the resolution of the sensor were not higher than the exhibited minimum pressure gradient of the system.

- Depth of the sample: Increasing the depth of the sample would reduce the minimum pressure gradient, thus reducing the number of data points that were different in value for a given ΔP.

3.1.2 Pressure decay system set up

As a first step, displacement measurement laser sensor was procured from Keyence. The laser would track the changes in the sample depth, occurring due to diffusion of carbon dioxide into the melt. This laser sensor had specific laser field criteria. As the pressure decay cell was built to suite the laser field, it would be better to start with the introduction of the laser field and the sensor.

Keyence® LKG laser sensor: The Keyence LKG laser sensor was selected on the basis of its capability of self-calibration and tracking of polymer surface movements with an accuracy of 10 microns. For any changes in depth below 10 micron it was decided to test the solution for its sensitivity to sample depth change of 10 micron. When the laser senses a point on any surface that point sends out reflections and the intensity of this image within certain angle is used by the LKG to give the position of that point with respect to the virtual zero on the laser scale. Before moving on with the experimental set up it would be appropriate to know in brief about the laser area diagram of the laser sensor as given in Figure [3.1].

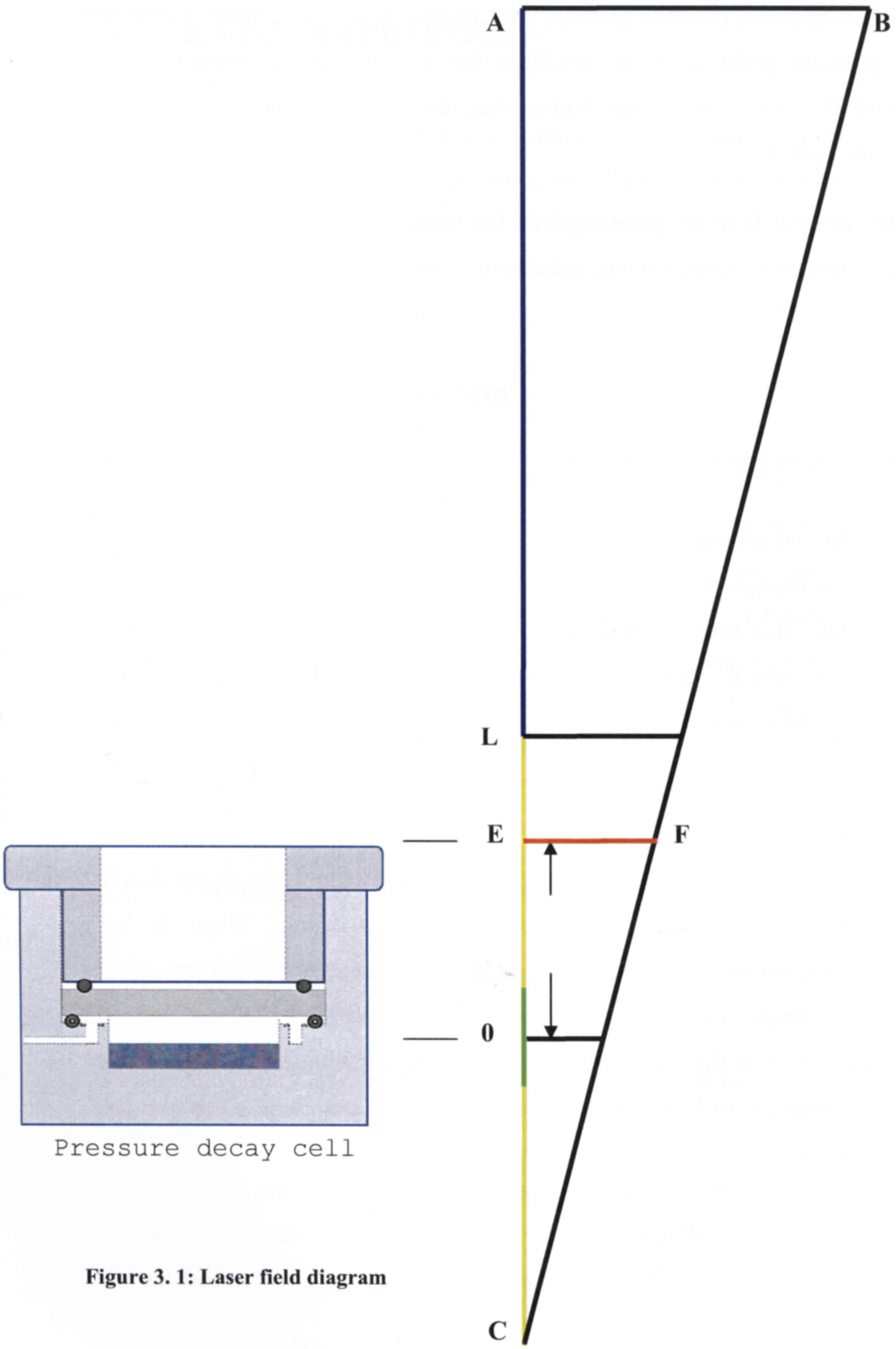

Figure 3. 1: Laser field diagram

- The functional area of the laser can be depicted as an inverted right triangle with the base 'AB' of 11 cms.
- Minimum distance of vision, the blue line 'AL' indicated on the diagram, is the minimum required focal distance between the point 'A' and the object surface to be watched by the laser.
- Vision span indicated by the yellow line 'LC' is the distance within which the laser beam can map movements effectively.
- The high precision region indicated by a green line is the region, where in the sample surface must be positioned to achieve the above said precision in measurement.
- Point '0' is the virtual zero on the displacement scale. Any displacement in the vision span would be mapped with respect to the virtual zero.

Pressure decay cell dimensions: The pressure decay cell dimensions were arrived upon with the help of the vision triangle as follows:

- Maximum thickness of glass window T_{max} across which the laser would maintain its accuracy was 10 mm.
- Maximum experimental pressure P_{max} was 1232 kPa.
- Maximum diameter of the high pressure - high temperature Borosilicate flat glass of above thickness T_{max}, capable of withstanding the experimental pressure, at experimental temperature was $d_{max} = 60\text{mm}$.
- The maximum diameter of the sample was 23 mm less than d_{max}. The breadth of 23 mm was consumed by the resting collar, the sealing assembly for the glass and the inlet gas dispersion channel. Thus the maximum available diameter for the sample was 37 mm.

- This 37 mm segment when placed parallel to the base line 'AB' of the vision triangle such that its ends rested on the remaining two sides of the triangle, the red line 'EF' in Figure [3.1]. The distance between the point 'E' and the virtual zero on the laser scale at point '0', would be the total height of the pressure cell upward from the polymer- gas interface.

- According to the permitted pressure cell height fixed by the vision triangle and the design pressure of 4882 kPa, a pressure decay cell with stainless steel body and a screw top along with view window of 37 mm diameter and the internal volume of 12.3 ml was built as shown in the Figure [3.2]. The actual pressure decay cell is shown in Figure [3.3].

- The depth to diameter ratio of the sample was to be maintained between 0.1- 0.2.

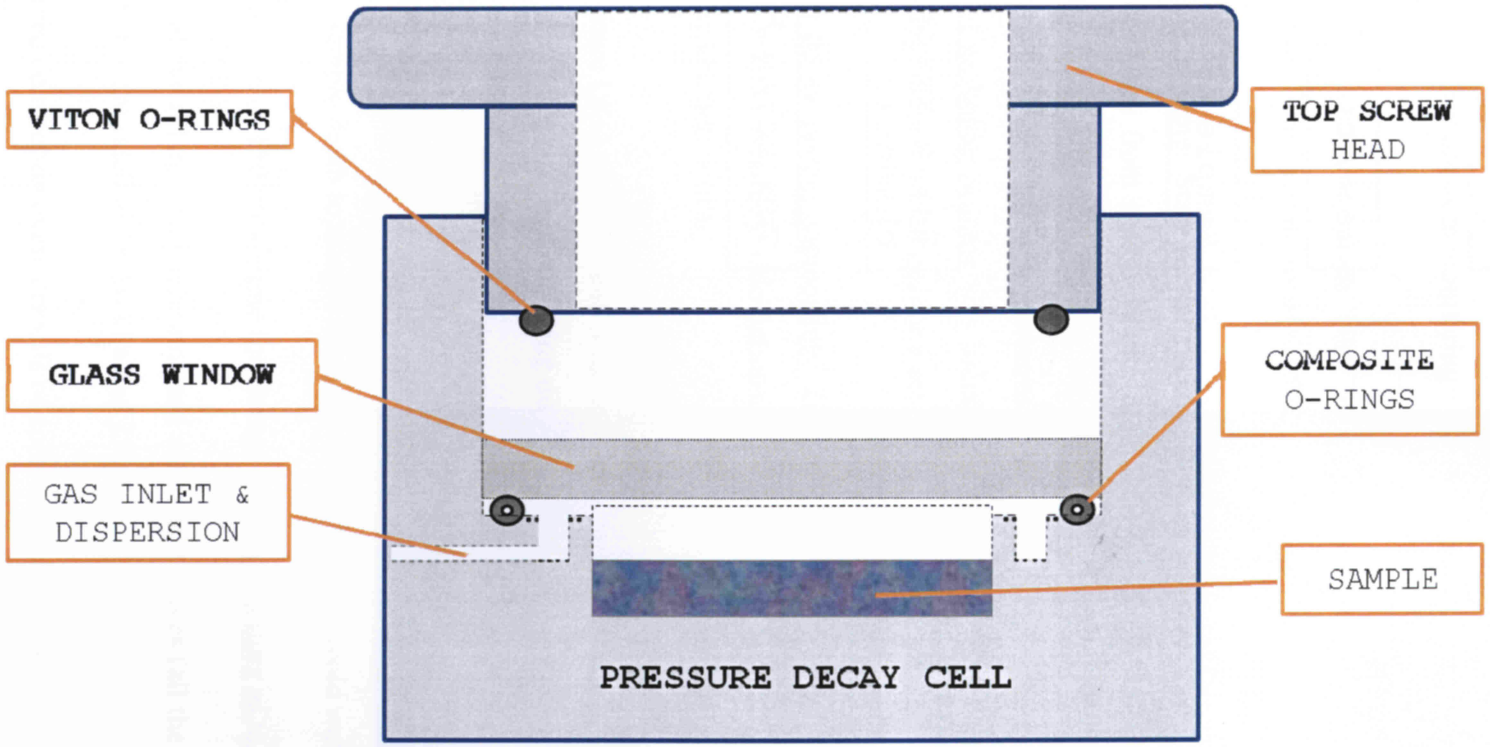

Figure 3. 2: Pressure decay cell - schematic

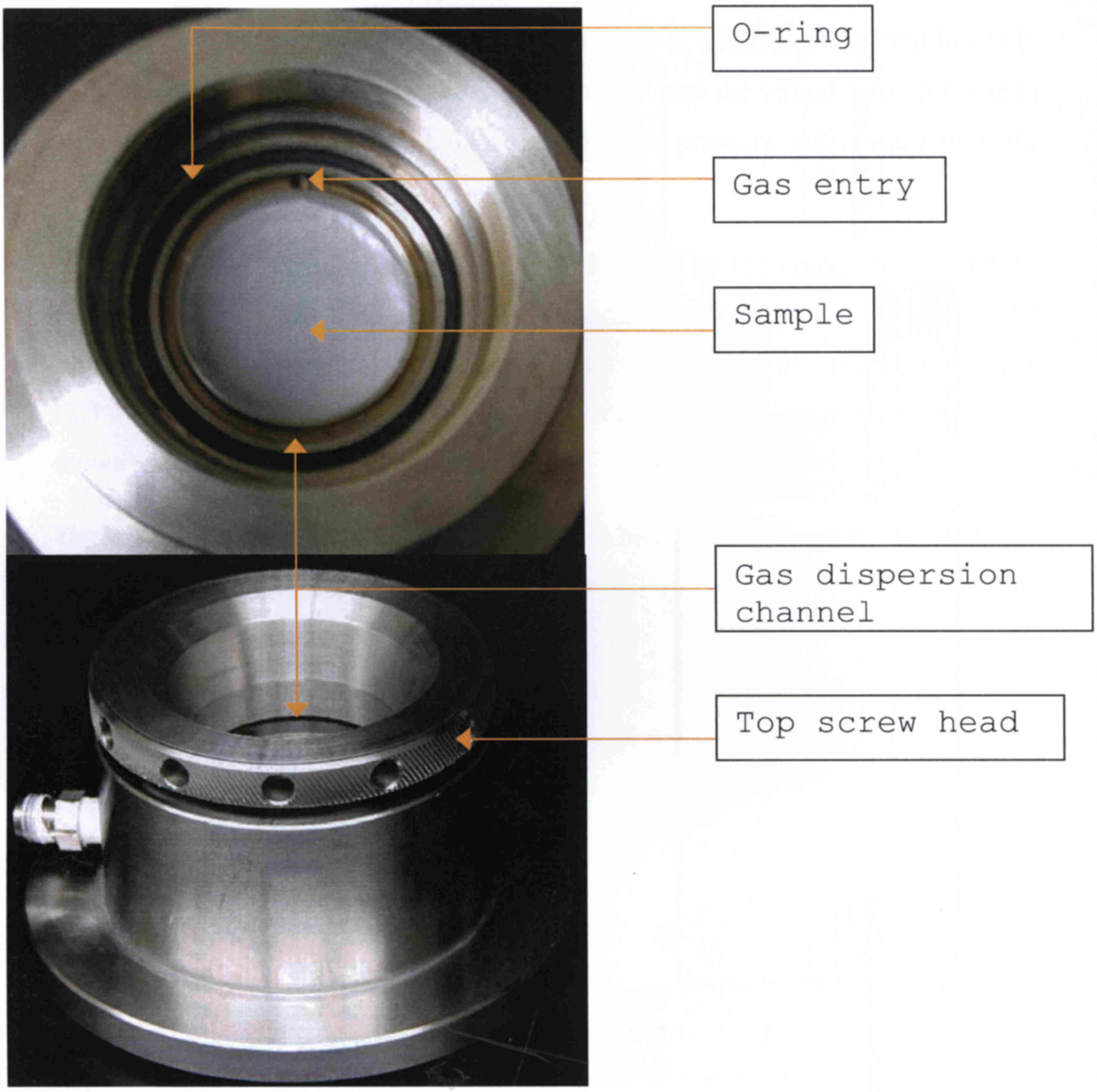

Figure 3. 3: Pressure decay cell – inside and out

Pressure sensor and transmitter: 2000 series Digiquartz®, intelligent pressure transmitter (±0.006 kPa) with variable data collection frequency and built in temperature correction was procured for pressure monitoring.

Oven: A forced circulation oven provided the isothermal environment with the temperature control capability of ±0.5°C.

Gasholder volume: Start of the pressure decay experiment required expanding of the conditioned gas from a capsule into the pressure decay (PD) cell. To arrive at a close estimate on the gasholder volume, experiments were conducted with carbon dioxide gas at 120°C and at four different pressures covering the pressure range of actual experiment. 150ml of gasholder volume was found suitable for pressurizing the pressure decay cell and storing of conditioned gas for a set of experiments.

Pressure decay system components: To summarize, the conducted pre-trial experiments and the related auxiliary calculations, resulted into a pressure decay system with the following characteristics:

- Keyence LKG displacement measurement sensor (10 microns) to track the changes in the melt sample depth, occurring due to diffusion of carbon dioxide into the melt.
- Pressure decay cell: with a view window, sample slot of 37 mm diameter and a gas dispersion channel.
- The sample depth to sample diameter ratio of 0.14 to avoid wall effects in diffusion.
- Gasholder of 150 ml volume for storage and conditioning of the gas.
- The above set up was interconnected with three valves (all the accessories used in the system were rated to 13790 kPa and 250°C).
- Forced convection oven, capable of controlling temperature up to ±0.5°C.

- 2000 series Digiquartz®, intelligent pressure transmitter (±0.006 kPa) and sampling frequency of 1.2 seconds for pressure decay measurement

Material: The polymer used in this experiment was a commercial grade low-density polyethylene as is from Nova Chemicals (Sarnia plant). Mw: 107500, Mz: 299800 and PDI: 5.21 was used. Carbon dioxide was of 99% purity from British Oxygen.

3.2 Experimental procedure

A schematic of the experimental setup used for the pressure decay technique is shown in Figure [3.4].

- Assembly and Pressure testing: The pressure decay system along with the filled gasholder is assembled inside the oven with the Swagelok fittings and is pressure tested at experimental temperature and 1.25 time the experiment pressure. The laser sensor is positioned on the oven top so as to get a complete view of the polymer inside.

- Sample preparation: During sample preparation, vacuum pump is connected to the system through valve 'C'. Valve 'A' and 'B' remain close and open respectively. LDPE granules are placed in the sample slot and melted under vacuum to form a melt slab of uniform thickness.

- Sample hold: After sample preparation, valve 'B' is closed and valve 'A' is opened. The pressure cell is maintained at experimental temperature under vacuum for a span of 8 hrs. Above hold helps uniform heat up of the gas in the gasholder, as well as conditioning of the sample.

- Pressure decay: Before starting the pressure decay the laser sensor recording is started, with the base reading of the polymer melt surface. At the start of the experiment valve 'C' is closed, then simultaneously valve 'B' is opened and valve 'A' is closed to pressurize and isolate the pressure decay cell from the gasholder. The

pressure decay starts 10 ± 2 seconds after the valve 'C' is closed. As pressure decay proceeds the pressure gradient with respect to time reduces and eventually the pressure in the sample chamber almost stabilizes. This is the point at which the carbon dioxide weight fraction in polymer sample reaches it's equilibrium value thus completing the pressure decay experiment. The pressure and laser measurements with time are acquired automatically by the data acquisition system.

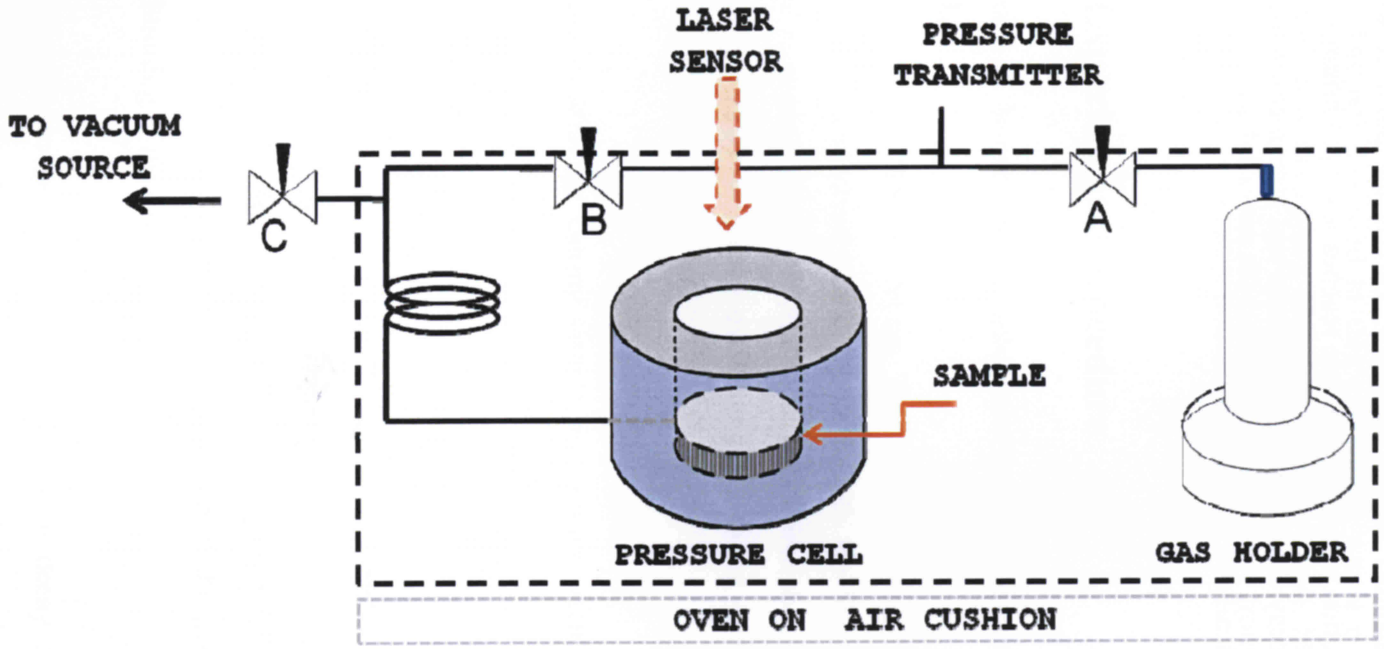

Figure 3. 4: Pressure decay setup – schematic experimental procedure

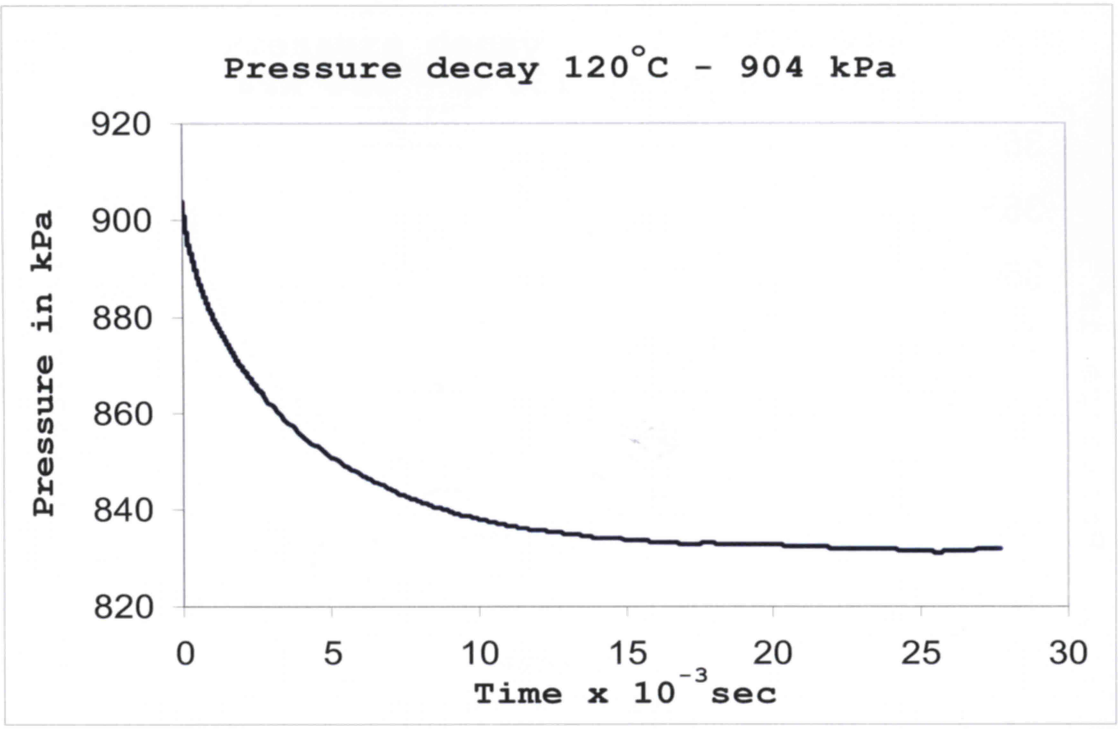

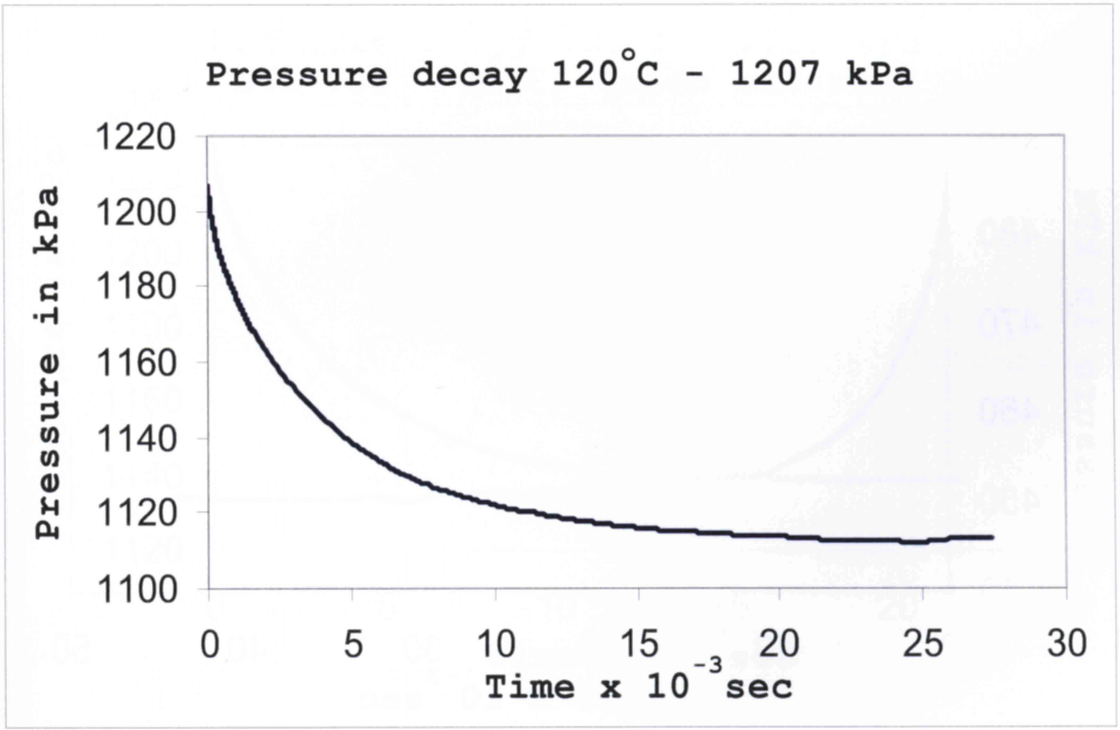

Figure 3. 5: Pressure decay sample plots at 120°C

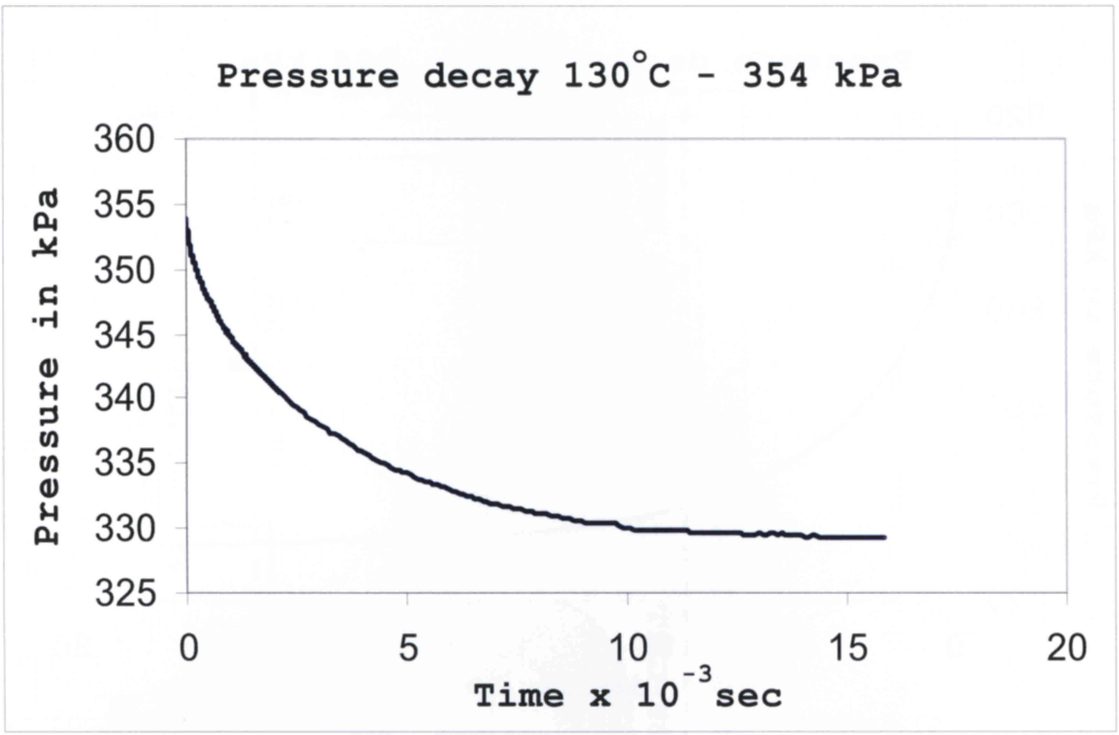

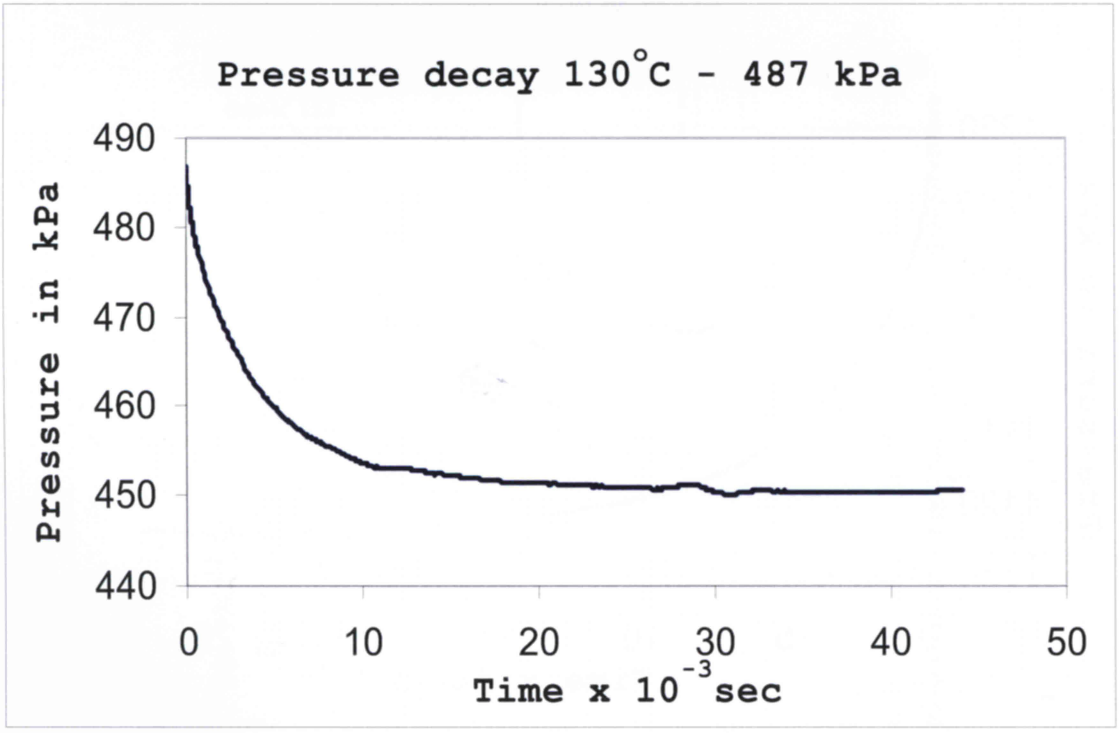

Figure 3. 6: Pressure decay sample plots at 130°C

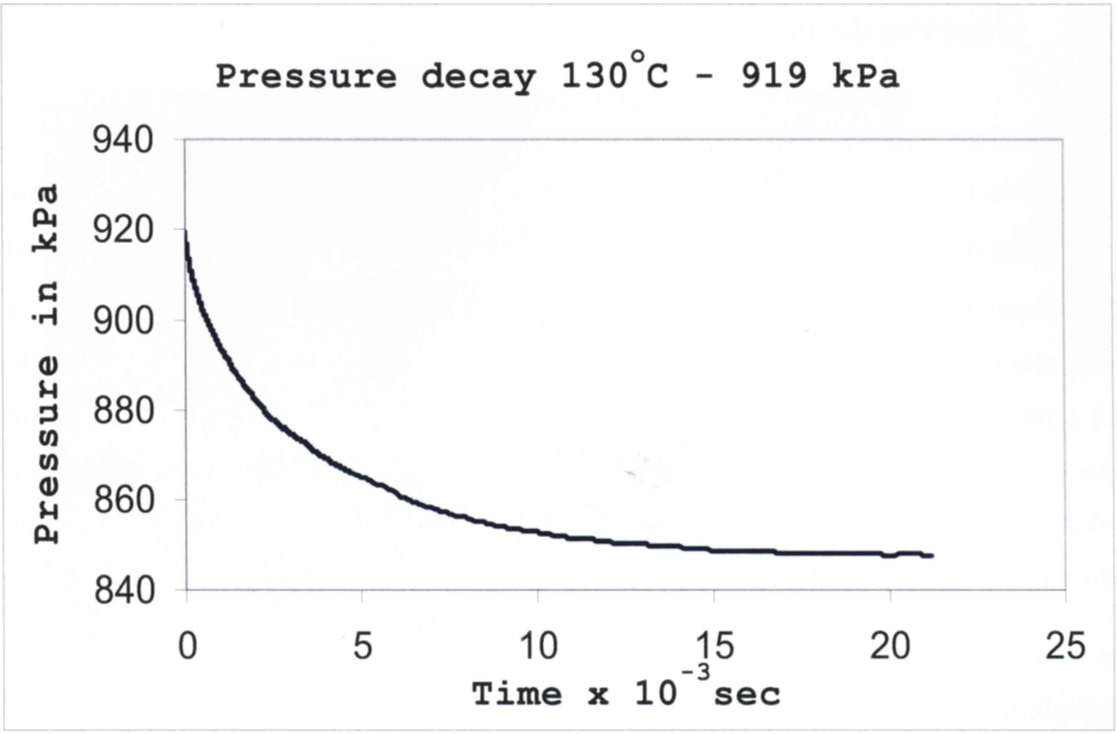

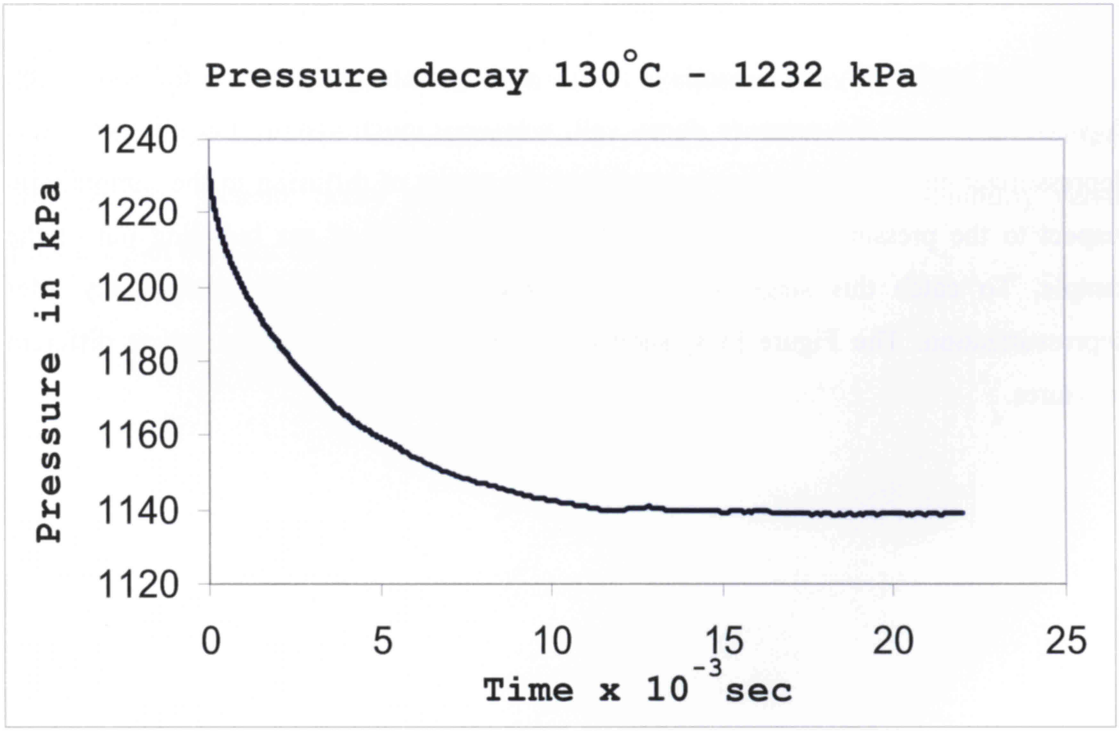

Figure 3. 7: Pressure decay sample plots at 130°C

3.3 Observations

The data from the pressure decay experiments Figures [3.5]–[3.7] indicates continuous pressure decay curves with decreasing value of ΔP, which eventually becomes negligible and further down gives a steady equilibrium pressure at which the ω_{sat} for LDPE melt at that temperature is obtained. The total ΔP achieved in a pressure decay experiment at a particular temperature increases as the experimental pressure increases. This is parallel to the already known observations made in published literature.[26] Similarly, decrease in total ΔP is observed with increase in temperature particularly at higher pressures, which indicates that solubility decreases with increase in melt temperature, which also is in line with the literature. [26,27]

As stated earlier, when the sample reaches saturation the pressure drop becomes negligible and the experiment as well as the data collection is stopped. There after the cell is isolated from the system and depressurized.

Due to the availability of a window on the cell, gas stripping out of the sample on depressurization of the pressure decay cell, was very much visible. On observing this depressurization carefully it was noticed that the extent of diffusion in the sample with respect to the pressure was also evident from the amount of gas bubbling out of the sample. To catch this stage, pressure decay cell was quenched immediately after depressurization. The Figure [3.8] shows the samples with entrapped gas at different pressures.

Figure 3. 8: Gas entrapped in quenched samples at different pressures

The pressure decay data obtained from the experiment were used in solving the continuity Equation (4.1) to calculate the values of $\omega(z,t)$. The initial and final pressures from several pressure decay experiments were used to generate a solubility versus pressure plot used for calculation of ω_{sat}.

4 Model development

Summary: In this chapter the determination of gas diffusivity from the pressure decay experiments is presented as an optimal control problem.[27] The aim is to arrive at the optimal diffusivity functional that will give the diffusivity at which the experimental mass of gas absorbed will be equal to the mass of gas absorbed obtained from the model. As stated earlier a unidirectional mass transfer model is described for the experimental process.

For a given gas diffusivity, it is needed to calculate the mass of gas diffused in LDPE. To determine its experimental value, the experimental pressure data are utilized. For some optimal gas diffusivity, the calculated and the experimental masses of the diffused gas would become equal. The conditions that are necessary for that optimality are derived. Finally, a numerical algorithm is outlined to compute the diffusivity of gas as function of its concentration in LDPE.

Experiments carried out in the manner stated earlier, resulted into a pressure decay where the system pressure decreased monotonically with time, correspondingly increasing the mass of the gas diffused in LDPE. Given enough time, as shown in Figure [3.5]–[3.8], the pressure would tend to an asymptotic value, as the LDPE approaches its gas-saturation limit.

4.1 The mass transfer model

The unidirectional mass transfer model as shown in Figure [4.1] implements the law of conservation of mass through equation of continuity. The process of mass transfer in the experiments satisfies the following conditions:

- The pressure decay was monitored by pressure sensor and transmitter (±0.006 kPa) and in a forced convection temperature control environment isothermal to the extent of ±0.5°C.
- Diffusion through the sample medium is the rate-determining step.
- There is no mass transfer of LDPE melt or light ends into the gas phase.
- Mass transfer of gas into LDPE melt is solely due to molecular diffusion.
- The chance of thermally induced convection currents in the LDPE melt phase can be precluded because the temperature of the pressure vessel is kept uniformly constant within ±0.5°C.
- The dissolution of carbon dioxide does not increase the LDPE melt density, so there is no possibility, whatsoever, of density-induced convection currents in the LDPE melt phase.
- There was no vibrating equipment in the experimental apparatus, which makes the chances of diffusion by bulk motion very remote. To avoid any effect of external vibrations, the apparatus is also placed over air cushions.
- Since the melt sample adheres to the chamber base and sidewalls, it can be assumed that diffusion through the slab occurs uniformly and is unidirectional, only through the top exposed surface of the melt.
- The concentration gradient is only along the depth of the LDPE melt layer, i.e., the z direction.
- The absorption of gas in LDPE melt is purely physical phenomenon.
- All changes in the permeant pressure are due to the mass absorption by the polymer.

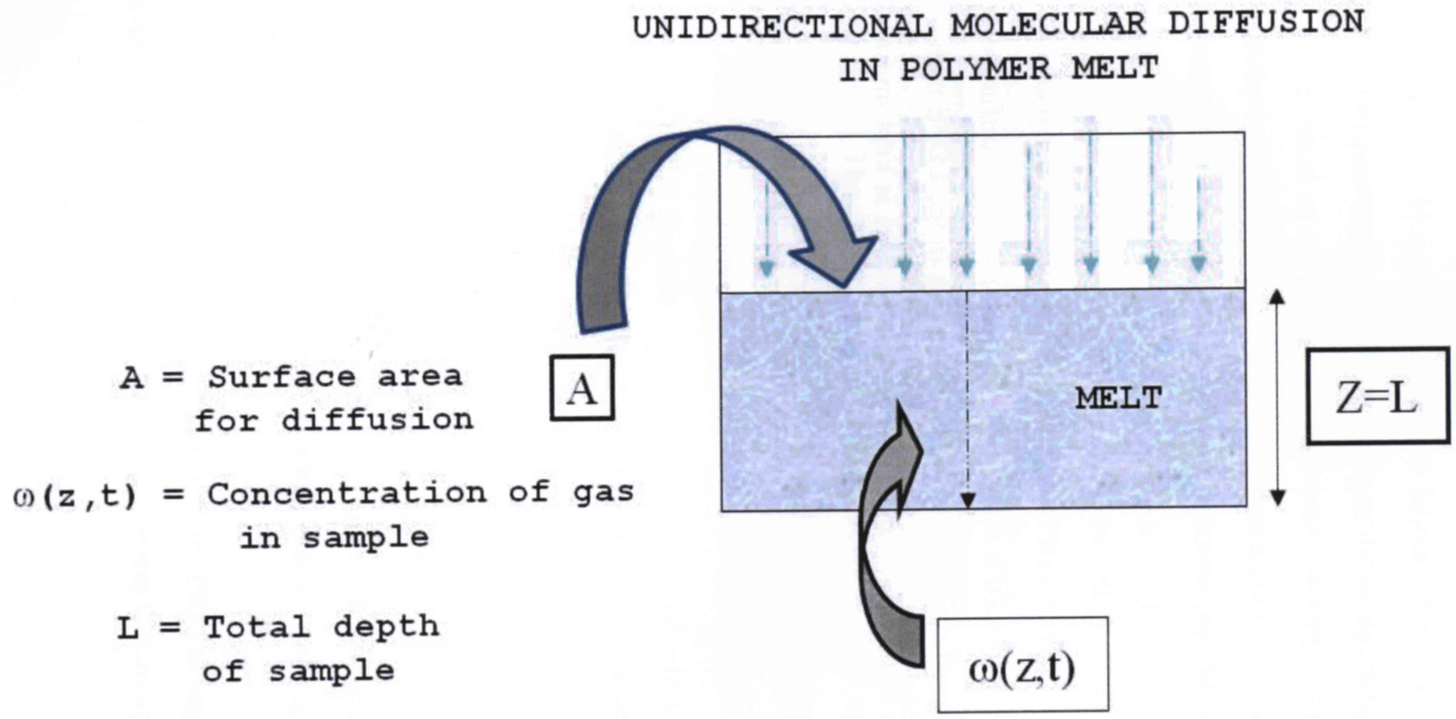

Figure 4. 1: Mass transfer model

The continuity equation: In the aforementioned experiments, the laser sensor did not detect any swelling of polymer samples. This fact implies that due to very low solubility, the amount of the gas absorbed in the polymer has a negligible effect on polymer density. Based on the above assumptions and the mass transfer model, the equation of continuity for the gas diffusing into the LDPE melt phase can be written as

$$\frac{\partial \omega}{\partial t} = D\left[1+\frac{\omega}{\rho_P}\right]\frac{\partial^2 \omega}{\partial z^2} + \left[\left(1+\frac{\omega}{\rho_P}\right)\frac{\partial D}{\partial \omega} + \frac{D}{\rho_P}\right]\left(\frac{\partial \omega}{\partial z}\right)^2 \equiv f \tag{4.1}$$

Where $\omega = \omega(z,t)$ is the mass fraction of the gas in the polymer at a depth z, and a time t. The diffusivity D depends on ω so that it is the composite function, $D = D[\omega(z,t)]$. Since there is no gas in the polymer at $t = 0$,

$$\omega(z,0) = 0 \quad \forall z: \quad 0 < z \le L \tag{4.2}$$

The interfacial gas concentration:

As the pressure decay proceeds the time derivatives of pressures keep reducing and eventually as the pressure stabilizes the concentration of solute gas reaches its equilibrium concentration at that temperature and pressure, for that medium of polymer. This mass concentration ω_{sat} is also the concentration that exists at the interface at the corresponding temperature and pressure and which can be expressed as

$$\omega(0,t) = \omega_{sat}(t) \qquad \forall t: \quad 0 \le t \le T \tag{4.3}$$

Because there is no mass transfer at the bottom of the cell,

$$\left.\frac{\partial \omega}{\partial z}\right|_{z=L} = 0 \qquad \forall t: \quad 0 \le t \le T \tag{4.4}$$

Equations (4.2 - 4.4) are the initial and boundary conditions for Equation (4.1).

4.2 Model development

As stated earlier the objective is to obtain an expression for diffusivity as a functional with the criteria that the calculated mass of gas absorbed obtained from the above diffusivity function must be equal to the experimentally obtained mass of gas diffused into the LDPE melt.

The square of difference between the mass of gas absorbed obtained from the above model and the experimental mass of gas absorbed can be mathematically expressed as follows:

$$I = \int_0^T \left[m_{\mathrm{gp,m}}(t) - m_{\mathrm{gp,e}}(t) \right]^2 \mathrm{d}t \tag{4.5}$$

Where T is the final time. At any time t, $m_{\mathrm{gp,e}}(t)$ is the experimental mass of gas absorbed in the polymer (Calculation procedure in Appendix A), while $m_{\mathrm{gp,m}}(t)$ is the model-predicted gas mass absorbed in polymer given by

$$m_{\mathrm{gp,m}}(t) = \int_0^L \omega(z,t)\rho_{\mathrm{mix}} A \mathrm{d}z \tag{4.6}$$

In the above equation, L is the depth of the polymer phase having a cross-sectional area A, and ρ_{mix} is the density of the gas-polymer mixture. Combining the Equations (4.5 - 4.6) generates the following expression for I:

$$I = \int_0^T \left[\int_0^L \omega \rho_{\mathrm{mix}} A \mathrm{d}z - m_{\mathrm{gp,e}} \right]^2 \mathrm{d}t \tag{4.7}$$

Here $\omega(z,t)$ is given by the Equation (4.1) for mass balance. Equation (4.1) can also be expressed as:

$$G(z,t)=\frac{\partial\omega}{\partial t}-f\left(\omega,\frac{\partial\omega}{\partial z},\frac{\partial^2\omega}{\partial z^2},D\right)=0 \tag{4.8}$$

Now the model development task can be expressed as follows:

The objective function given by Equation (4.7) is to be minimized taking into consideration the constraint lay down by Equation (4.1).

Because G is nonlinear partial differential equation, with the boundary condition - Equation (4.3), as a set of discrete values, an adjoint variable, $\lambda(z,t)$ is needed. The adjoint variable would incorporate the constraint of Equation (4.1) into Equation (4.7) to yield an augmented objective functional.

$$K=I+\int_0^T\int_0^L\left[\lambda(z,t)G(z,t)\right]\mathrm{d}z\mathrm{d}t \tag{4.9}$$

Where I represents Equation (4.7)

Equation (4.9) has transformed the above task of minimization with constraint to minimization without constraint.

Optimality criterion: Minimization of the difference between experimental and model mass of gas absorbed is equivalent to minimization of K given by Equation (4.9). For minimization of K, its first variation δK is forced to zero.

Forcing each term in the expression for δK to zero gives rise to following variation derivative:

$$J=-\lambda\frac{\partial f}{\partial D}=0;\quad 0\le z\le L,\quad 0\le t\le T \tag{4.10}$$

Along with the criteria:

$$\delta\omega(z,0)=0 \qquad \forall z: \quad 0\le z\le L \tag{4.11}$$

$$\lambda(z,T)=0 \qquad \forall z: \quad 0\le z\le L \tag{4.12}$$

$$\delta\omega(0,t)=0 \qquad \forall t: \quad 0\le t<T \tag{4.13}$$

$$\left[\lambda\frac{\partial f}{\partial\omega_z}-\frac{\partial}{\partial z}\left(\lambda\frac{\partial f}{\partial\omega_{zz}}\right)\right]_{z=L}=0 \tag{4.14}$$

Where $\omega_z\equiv\dfrac{\partial\omega}{\partial z}$, and $\omega_{zz}\equiv\dfrac{\partial^2\omega}{\partial z^2}$

$$\left[\lambda\frac{\partial f}{\partial\omega_{zz}}\right]_{z=0,L}=0 \tag{4.15}$$

$$\frac{\partial\lambda}{\partial t}=2(m_{\text{gp,m}}-m_{\text{gp,e}})\rho A-\lambda\frac{\partial f}{\partial\omega}+\frac{\partial}{\partial z}\left(\lambda\frac{\partial f}{\partial\omega_z}\right)-\frac{\partial^2}{\partial z^2}\left(\lambda\frac{\partial f}{\partial\omega_{zz}}\right) \tag{4.16}$$

(The detail derivation for the above conditions is given in the next section)

Using Equation (4.1 and 4.7) Equation (4.16) can be written as

$$\begin{aligned}\frac{\partial\lambda}{\partial t}&=2\rho A\left(m_{\text{gp,m}}-m_{\text{gp,e}}\right)+\frac{\lambda}{\rho}\frac{\partial D}{\partial\omega}\left(\frac{\partial\omega}{\partial z}\right)^2\\&\quad+\left(1+\frac{\omega}{\rho}\right)\left[\lambda\frac{\partial D}{\partial\omega}\frac{\partial^2\omega}{\partial z^2}+\lambda\frac{\partial^2 D}{\partial\omega^2}\left(\frac{\partial\omega}{\partial z}\right)^2-D\frac{\partial^2\lambda}{\partial z^2}\right]\end{aligned} \tag{4.17}$$

The above equation has the following Equation (4.12) as its initial condition,

$$\lambda(z,T)=0 \qquad \forall z: \quad 0 \le z \le L$$

Equation (4.1, 4.4, 4.14) yield

$$\left.\frac{\partial \lambda}{\partial z}\right|_{z=L} = 0 \qquad \forall t: \quad 0 \le t \le T \tag{4.18}$$

Equation (4.1 and 4.15) yield

$$\lambda(0,t)=\lambda(L,t)=0 \qquad \forall t: \quad 0 \le t \le T \tag{4.19}$$

Above Equations (4.18) and (4.19) are the boundary conditions of Equation (4.17). Equation (4.10) is the necessary condition for minimization subject to satisfaction of the Equation (4.1) and (4.17)

4.3 Necessary conditions for optimality

The optimal control problem is to find the function $D(\omega)$ that minimizes the objective functional given by Equation (4.7) subject to the continuity equation, Equation (4.1), i.e.

$$G = \frac{\partial \omega}{\partial t} - f = 0 \tag{4.20}$$

where

$$f = D\left[1+\frac{\omega}{\rho}\right]\frac{\partial^2 \omega}{\partial z^2} + \left[\left(1+\frac{\omega}{\rho}\right)\frac{\partial D}{\partial \omega} + \frac{D}{\rho}\right]\left(\frac{\partial \omega}{\partial z}\right)^2 \tag{4.21}$$

The above problem is equivalent to the unconstrained minimization of Equation (4.9)

$$K = I + \int_0^T \int_0^L [\lambda(z,t) G(z,t)] \mathrm{d}z\mathrm{d}t \tag{4.9}$$

with $\lambda(z,t)$ as an adjoint variable.

Necessary Condition for the Minimum

The necessary condition for the minimum is that the variation in K is zero, i.e.

$$\delta K = \delta I + \int_0^T \int_0^L [\lambda(z,t) \delta G(z,t)] \mathrm{d}z\mathrm{d}t = 0 \tag{4.22}$$

In the above equation,

$$\delta I = \int_0^T 2(m_{\mathrm{gp,m}} - m_{\mathrm{gp,c}}) \int_0^L \rho A \delta\omega \mathrm{d}z\mathrm{d}t = \int_0^T \int_0^L 2(m_{\mathrm{gp,m}} - m_{\mathrm{gp,c}}) \rho A \delta\omega \mathrm{d}z\mathrm{d}t \tag{4.23}$$

and δG is given by

$$\delta G = \frac{\partial}{\partial t}(\delta\omega) - \frac{\partial f}{\partial \omega}\delta\omega - \frac{\partial f}{\partial \omega_z}\delta\omega_z - \frac{\partial f}{\partial \omega_{zz}}\delta\omega_{zz} - \frac{\partial f}{\partial D}\delta D \tag{4.24}$$

Substituting Equations (4.24) and (4.23) into (4.22) yields

$$\begin{aligned} \delta K = \int_0^T \int_0^L \Bigg[& \left\{ 2(m_{\mathrm{gp,m}} - m_{\mathrm{gp,c}}) \rho A \mathrm{d}z\mathrm{d}t - \lambda \frac{\partial f}{\partial \omega} \right\} \delta\omega \\ & + \lambda \left\{ \frac{\partial(\delta\omega)}{\partial t} - \frac{\partial f}{\partial \omega_z}\delta\omega_z - \frac{\partial f}{\partial \omega_{zz}}\delta\omega_{zz} - \frac{\partial f}{\partial D}\delta D \right\} \Bigg] \mathrm{d}z\mathrm{d}t = 0 \end{aligned} \tag{4.25}$$

Integration by parts of the third, fourth and fifth terms of the above equation yields

$$\int_0^T\int_0^L \lambda \frac{\partial(\delta\omega)}{\partial t}\,\mathrm{d}z\mathrm{d}t = \int_0^L \left\{ \left[\lambda\delta\omega\right]_0^T - \int_0^T \frac{\partial\lambda}{\partial t}\delta\omega\mathrm{d}t \right\}\mathrm{d}z \tag{4.26}$$

$$\int_0^T\int_0^L \lambda \frac{\partial f}{\partial \omega_z}\delta\omega_z\,\mathrm{d}z\mathrm{d}t = \int_0^T \left\{ \left[\lambda \frac{\partial f}{\partial \omega_z}\delta\omega \right]_0^L - \int_0^L \frac{\partial}{\partial z}\left(\lambda \frac{\partial f}{\partial \omega_z} \right)\delta\omega\mathrm{d}z \right\}\mathrm{d}t \tag{4.27}$$

$$\begin{aligned}\int_0^T\int_0^L \lambda \frac{\partial f}{\partial \omega_{zz}}\delta\omega_{zz}\,\mathrm{d}z\mathrm{d}t = \int_0^T \Bigg\{ &\left[\lambda \frac{\partial f}{\partial \omega_{zz}}\frac{\partial(\delta\omega)}{\partial z} - \frac{\partial}{\partial z}\left(\lambda \frac{\partial f}{\partial \omega_{zz}} \right)\delta\omega \right]_0^L \\ &+ \int_0^L \frac{\partial^2}{\partial z^2}\left(\lambda \frac{\partial f}{\partial \omega_{zz}} \right)\delta\omega\mathrm{d}z \Bigg\}\mathrm{d}t\end{aligned} \tag{4.28}$$

Substitution of Equations (4.26)–(4.28) into Equation (4.25) gives

$$\begin{aligned}\delta K = &\int_0^T\int_0^L \left\{ -\frac{\partial\lambda}{\partial t} + 2(m_{\mathrm{gp,m}} - m_{\mathrm{gp,e}})\rho A - \lambda\frac{\partial f}{\partial \omega} + \frac{\partial}{\partial z}\left(\lambda \frac{\partial f}{\partial \omega_z} \right) - \frac{\partial^2}{\partial z^2}\left(\lambda \frac{\partial f}{\partial \omega_{zz}} \right) \right\}\delta\omega\mathrm{d}z\mathrm{d}t \\ &- \int_0^T\int_0^L \lambda \frac{\partial f}{\partial D}\delta D\mathrm{d}z\mathrm{d}t + \int_0^L \left[\lambda\delta\omega\right]_0^T \mathrm{d}z + \int_0^T \left[\lambda \frac{\partial f}{\partial \omega_z} - \frac{\partial}{\partial z}\left(\lambda \frac{\partial f}{\partial \omega_{zz}} \right) \right]_{z=0} \delta\omega(0,t)\,\mathrm{d}t \\ &- \int_0^T \left[\lambda \frac{\partial f}{\partial \omega_z} - \frac{\partial}{\partial z}\left(\lambda \frac{\partial f}{\partial \omega_{zz}} \right) \right]_{z=L} \delta\omega(L,t)\,\mathrm{d}t - \int_0^T \left[\lambda \frac{\partial f}{\partial \omega_{zz}}\frac{\partial(\delta\omega)}{\partial z} \right]_0^L \mathrm{d}t = 0\end{aligned} \tag{4.29}$$

In the above equation, the first integral is eliminated by defining λ as given by Equation (4.16) below

$$\frac{\partial\lambda}{\partial t} = 2(m_{\mathrm{gp,m}} - m_{\mathrm{gp,e}})\rho A - \lambda\frac{\partial f}{\partial \omega} + \frac{\partial}{\partial z}\left(\lambda \frac{\partial f}{\partial \omega_z} \right) - \frac{\partial^2}{\partial z^2}\left(\lambda \frac{\partial f}{\partial \omega_{zz}} \right) \tag{4.16}$$

As stated earlier the above equation has the following final form:

$$\frac{\partial \lambda}{\partial t} = 2\rho A(m_{\text{gp,m}} - m_{\text{gp,e}}) + \frac{\lambda}{\rho}\frac{\partial D}{\partial \omega}\left(\frac{\partial \omega}{\partial z}\right)^2 + \left(1+\frac{\omega}{\rho}\right)\left[\lambda\frac{\partial D}{\partial \omega}\frac{\partial^2 \omega}{\partial z^2} + \lambda\frac{\partial^2 D}{\partial \omega^2}\left(\frac{\partial \omega}{\partial z}\right)^2 - D\frac{\partial^2 \lambda}{\partial z^2}\right] \tag{4.30}$$

Because the initial mass fraction of the gas in the polymer is known at the interface and is zero elsewhere, the variation $\delta\omega(z,0)$ is zero for all z. Since the final gas mass fraction is not specified, the third integral in Equation (4.29) is eliminated by forcing

$$\lambda(z,T) = 0; \qquad 0 \le z \le L \tag{4.12}$$

Since the equilibrium concentration of gas at the interface, $\omega(0,t) \equiv \omega_{\text{sat}}(t)$, is always specified $\delta\omega(0,t)$ is zero. Thus, the fourth integral is eliminated in Equation (4.29). Furthermore, by forcing

$$\lambda(L,t) = 0; \qquad 0 \le t \le T \tag{4.31}$$

The fifth integral in Equation (4.29) is eliminated. In addition to Equation (4.31), setting

$$\lambda(0,t) = 0; \qquad 0 \le t \le T \tag{4.32}$$

Eliminates the sixth integral in Equation (4.29). Note that Equation (4.12) is the final condition for Equation (4.30), which has Equations (4.31) and (4.32) as its two boundary conditions.

Hence, subject to Equations (4.12), (4.30)–(4.32), Equation (4.29) gets simplified to

$$\delta K = -\int_0^T \int_0^L \lambda \frac{\partial f}{\partial D} \delta D \mathrm{d}z\mathrm{d}t = 0 \tag{4.33}$$

Thus, at the minimum of K the variational derivative of K with respect to D is zero, and is given by Equation (4.10)

$$J = -\lambda \frac{\partial f}{\partial D} = 0; \quad 0 \le z \le L, \quad 0 \le t \le T \tag{4.10}$$

The negative of J provides the gradient correction for $D(\omega)$ in the iterative minimization of K.

4.4 Diffusivity calculation

The diffusivity was calculated by integrating Equation (4.1) with an initial guessed diffusivity, and storing the results for use in the backward integration of Equation (4.17). This exercise enabled the calculation of J, which is used to apply gradient corrections to the diffusivity. This procedure was repeated until there is no further reduction in I.

The calculation of I requires $m_{\mathrm{gp,c}}(t)$, which was obtained from the experimental pressure versus time data in conjunction with the PVT relationship of the gas (as given in appendix A). PVT data of CO_2 gas from Vergaftic was used for above calculation. The value of $m_{\mathrm{gp,c}}(t)$ at final pressure corresponding to the end of an experiment yields saturation mass fraction of gas, i.e. $\omega_{\mathrm{sat}}[P(t)]$. The $\omega_{\mathrm{sat}}[P(t)]$ plots as shown in Figure [5.11] for several experiments together provide the solubility database, which furnishes the boundary condition expressed by Equation (4.3).

Equation (4.1) and (4.17) were numerically integrated after applying Runga-Kutta-5 adoptive step size control method along z direction. The time period for the integrations was carefully selected to restrict pressure decay to less than 2% of the initial pressure.[28] The diffusivity was considered to be discrete function, $D(\omega)$, at specified gas mass fractions between zero and the maximum, at time $t = 0$, for an experiment. For best results, as several numerical experiments had indicated, $D(\omega)$ was initialized to a uniform value as high as possible without causing $m_{gp,m}(t)$ to cross $m_{gp,e}(t)$. Computations and fine-tuning of results was done with the help of a C++ program. During the computations, cubic splines were used to interpolate $D(\omega)$ as well as its first and second derivatives with respect to ω, $m_{gp,e}(t)$, $\omega_{sat}[P(t)]$, $\omega(t)$ at a given z, and $J(\omega)$ at each experimental time instant. The values of $J(\omega)$ were time-averaged before their usage for the gradient correction in $D(\omega)$ by Broyden-Fletcher-Goldfarb-Shanno.[29] The maximum correction in diffusivity was limited to 1% of its value to allow slow but steady approach to the minimum.

The parameters used in diffusivity calculations are listed in Table (4.1) below

Parameters	Values
Mass of polymer	6×10^{-3} kgs
Sample diameter	37×10^{-3} m
D initial guess	8×10^{-10} m^2/s
Diffusivity intervals	75
Grid points across sample depth	60

Table 4. 1: Parameters for diffusivity calculations

5 Results and conclusion

This section presents the analysis of data from pressure decay experiment conducted to determine the diffusion coefficient of carbon dioxide in low-density poly(ethylene) melt in the pressure range of 352 to 1232 kPa at 120°C and 130°C.

5.1 Results

As stated earlier the objective was to obtain an expression for diffusivity as a functional with the criteria that the calculated mass of gas absorbed obtained from the above diffusivity function must be equal to the experimentally obtained mass of gas diffused into the LDPE melt. To recapitulate, the above objective was achieved with minimization of the functional derived from difference in experimental and model mass of gas absorbed by polymer melt.

5.1.1 Objective function path

The Figures [5.1]–[5.4] shows the extent of functional minimization achieved in the course of obtaining optimal concentration dependent diffusivity. Minimum objective function values obtained during each trial run are listed in Table (5.1).

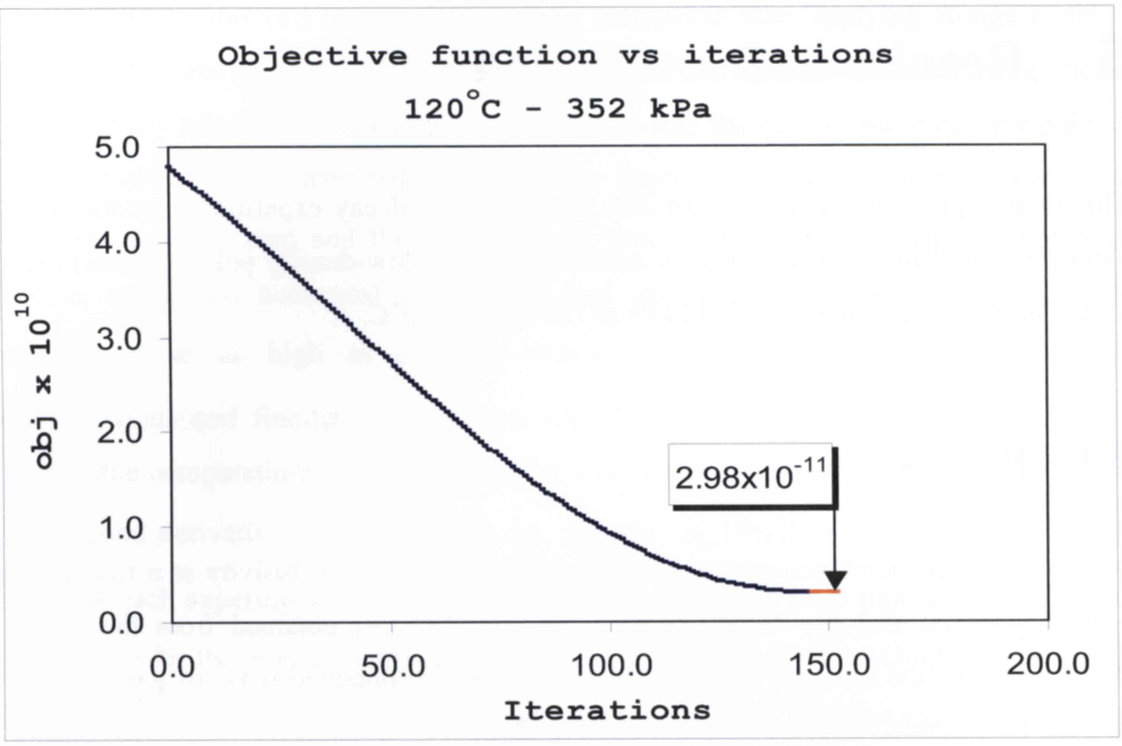

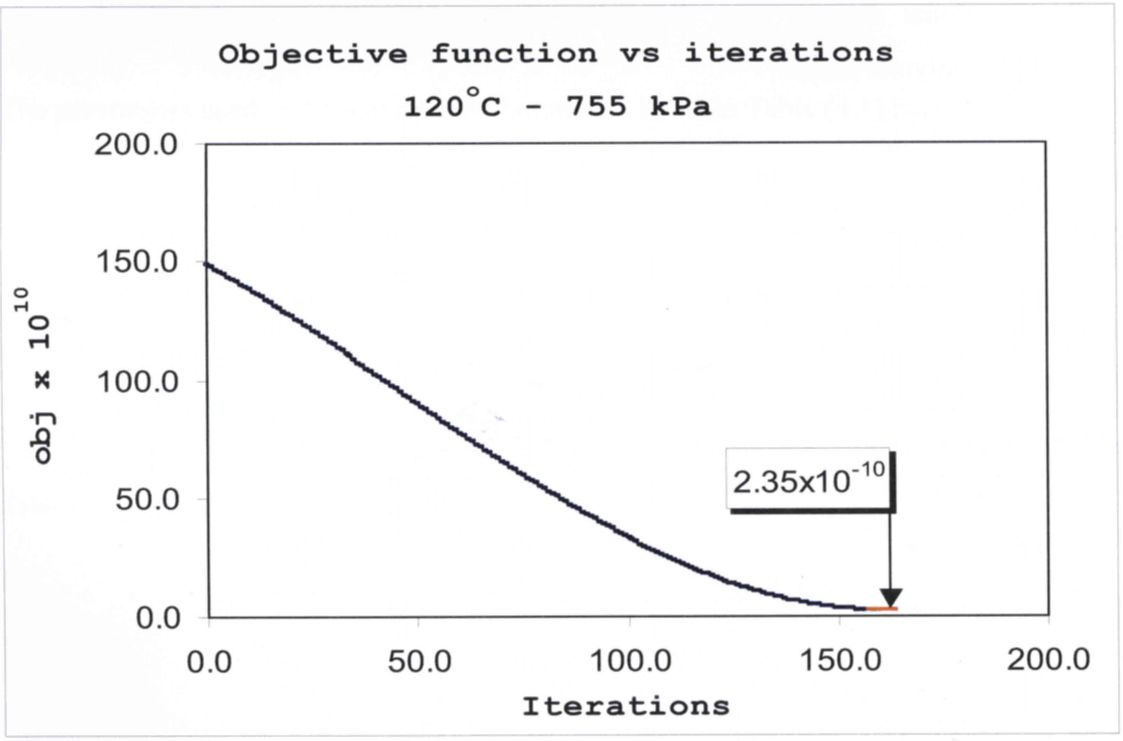

Figure 5. 1: Extent of minimization of objective function 352 kPa and 755 kPa at 120°C

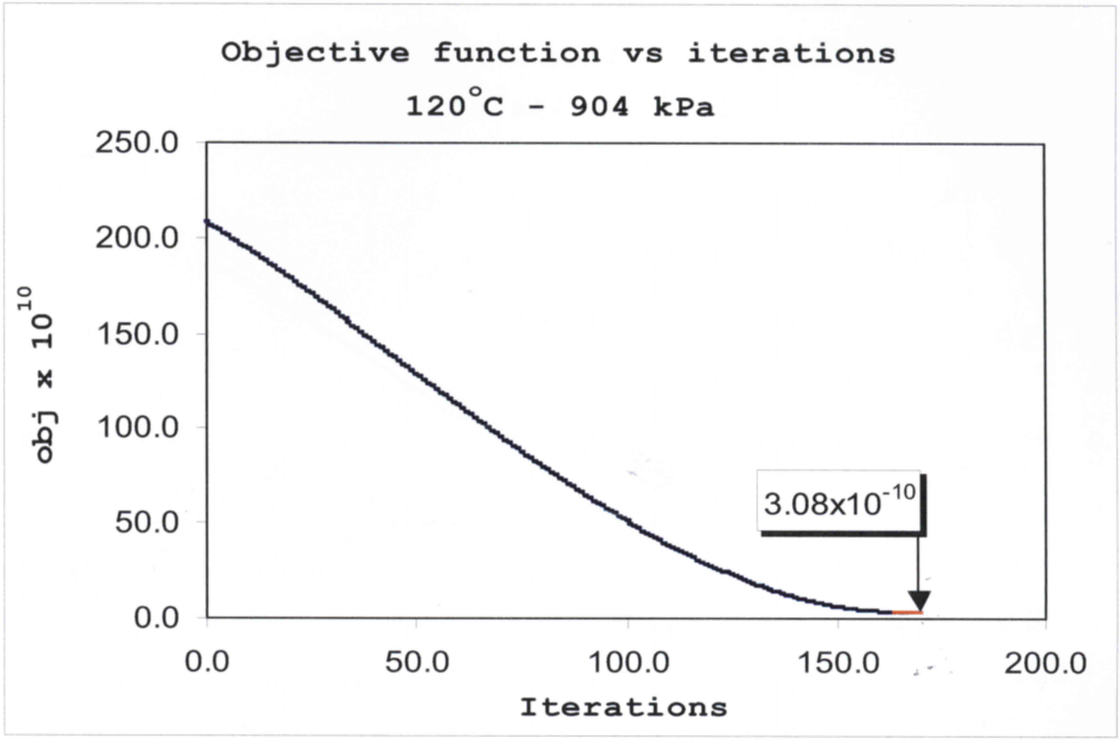

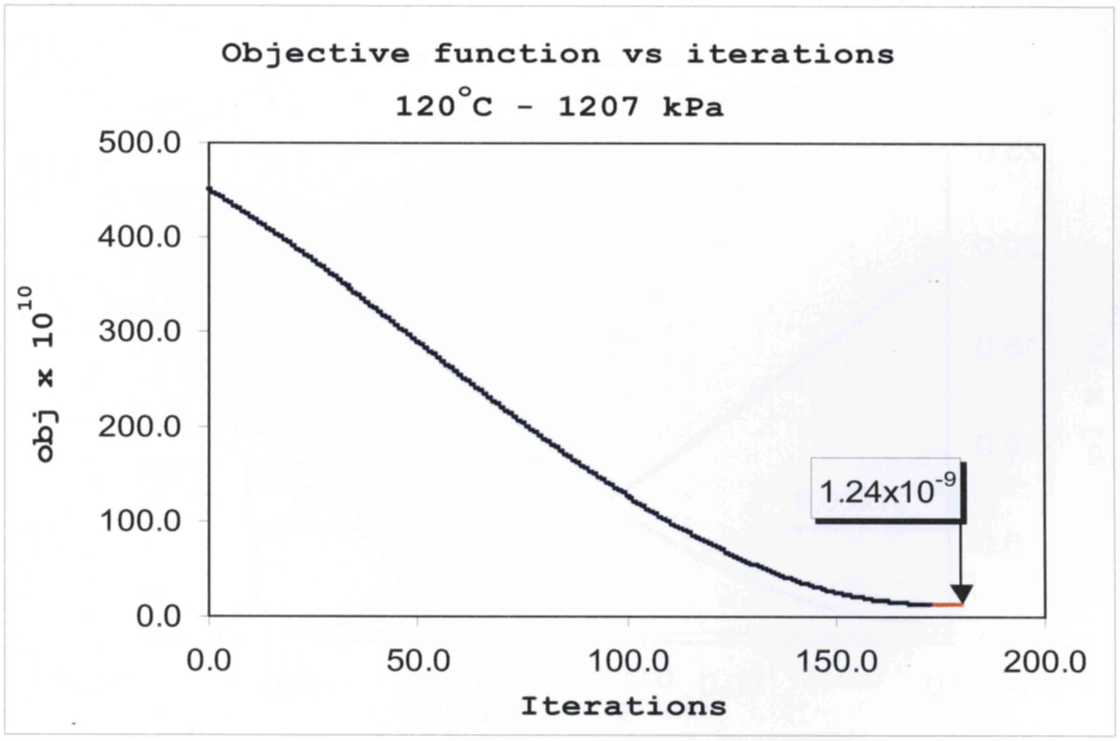

Figure 5. 2: Extent of minimization of objective function 904 kPa and 1207 kPa at 120°C

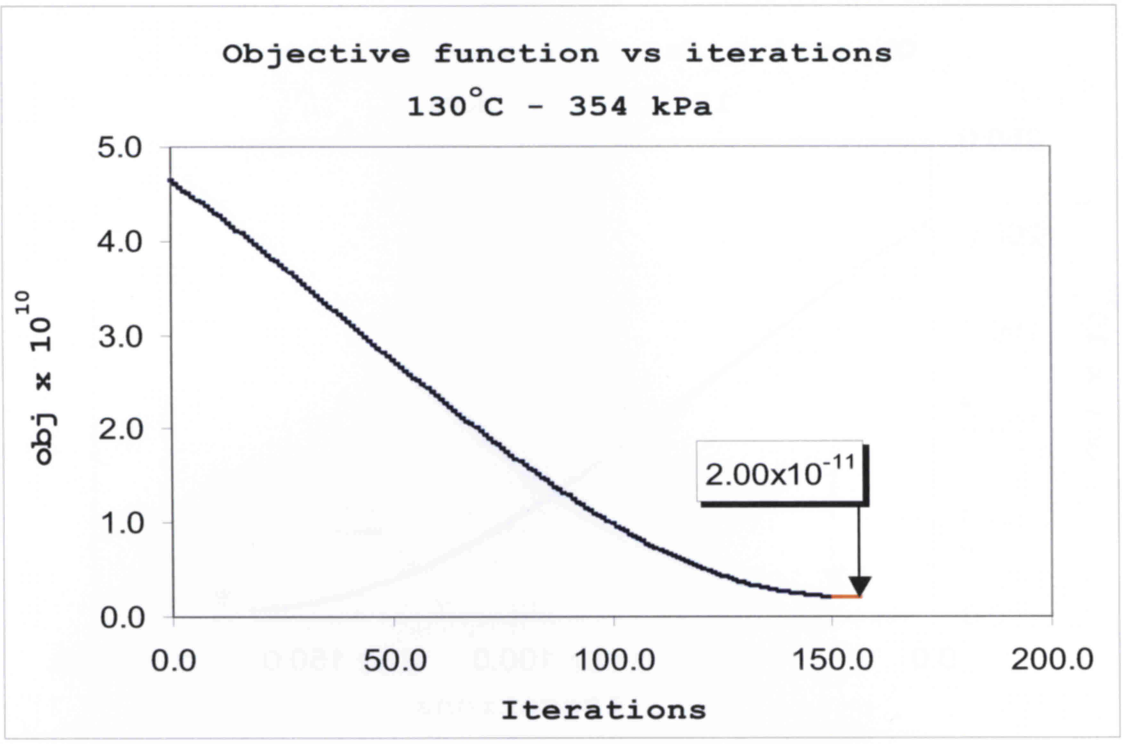

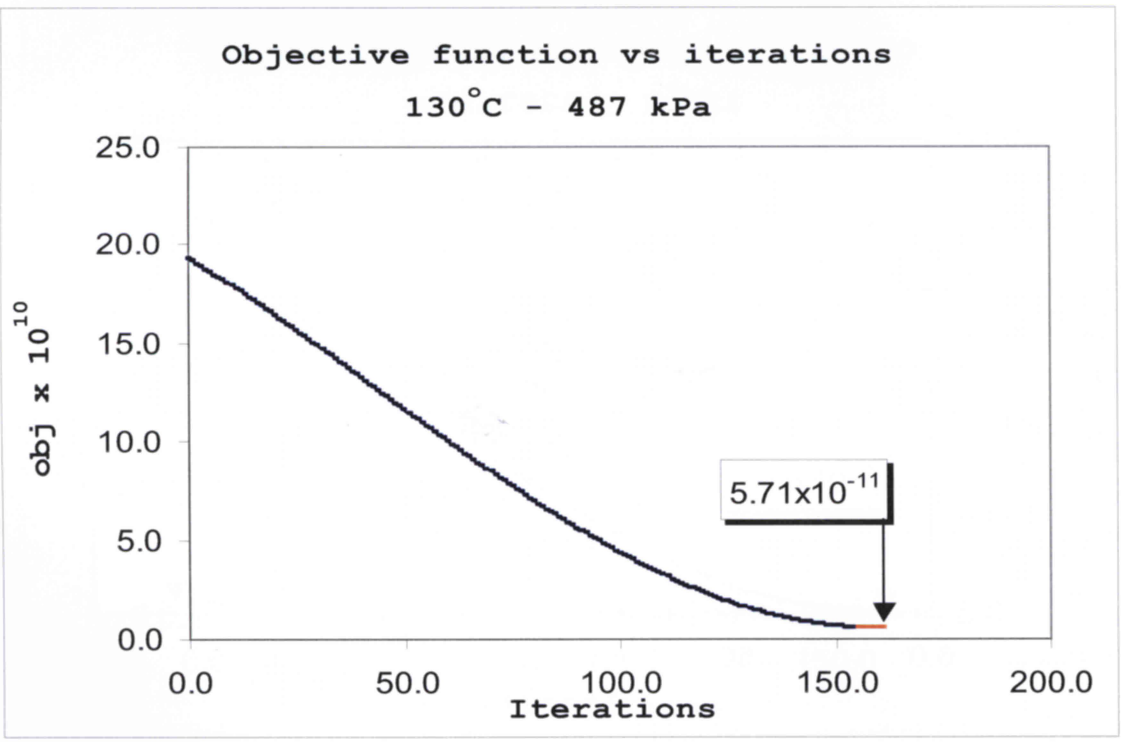

Figure 5. 3: Extent of minimization of objective function 354 kPa and 487 kPa at 130°C

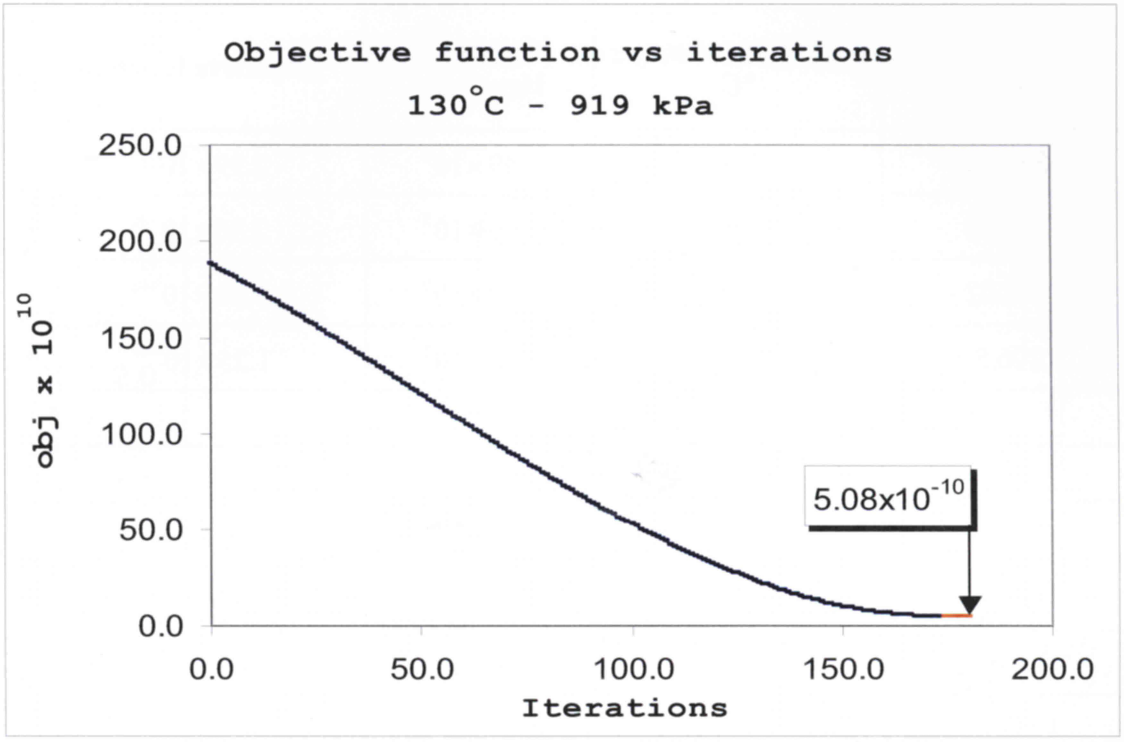

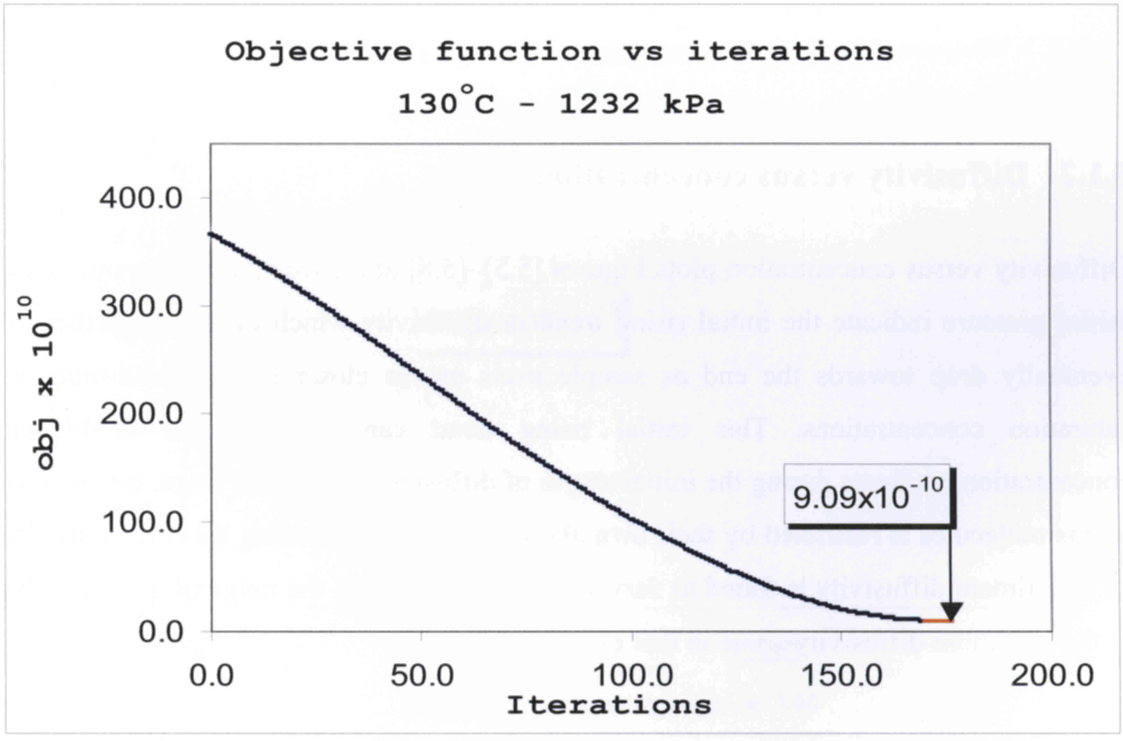

Figure 5. 4: Extent of minimization of objective function 919 kPa and 1232 kPa at 130°C

Pressure in kPa	Temperature °C	Number of Iterations	Objective function
351.92	120	1.49×10^{2}	2.99×10^{-11}
755.16	120	1.60×10^{2}	2.36×10^{-10}
904.02	120	1.67×10^{2}	3.09×10^{-10}
1206.86	120	1.77×10^{2}	1.25×10^{-09}
353.90	130	1.53×10^{2}	2.01×10^{-11}
486.83	130	1.58×10^{2}	5.72×10^{-11}
919.22	130	1.77×10^{2}	5.09×10^{-10}
1232.02	130	1.73×10^{2}	9.10×10^{-10}

Table 5. 1: Minimum objective function values

5.1.2 Diffusivity versus concentration

Diffusivity versus concentration plots Figures [5.5]–[5.8] at a particular temperature and initial pressure indicate the initial rising trend in diffusivity which evens off further to eventually drop towards the end as sample mass moves closer to its equilibrium or saturation concentrations. This initial rising trend can be attributed to higher concentration gradients during the initial stages of diffusion. In the later stage, the motion of gas molecules is restricted by their own abundance, thus decreasing the diffusivity. In an experiment diffusivity is found to vary with concentration in the range of 85% to 96% of the minimum diffusivity value in that experiment.

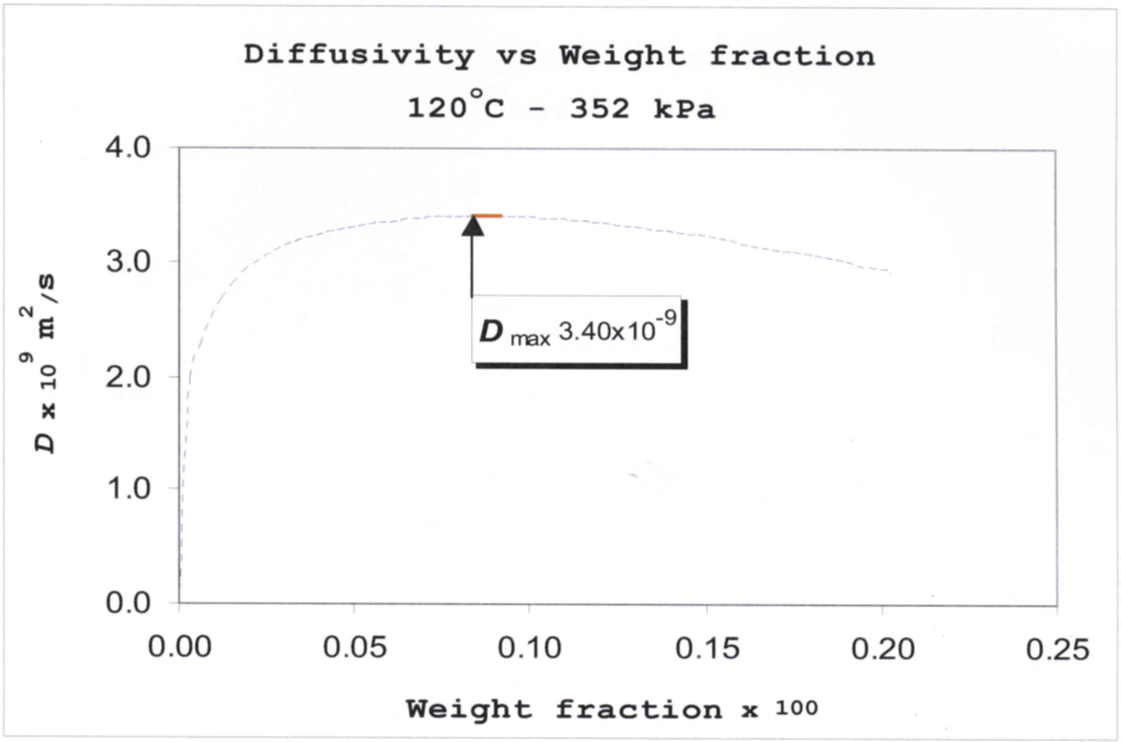

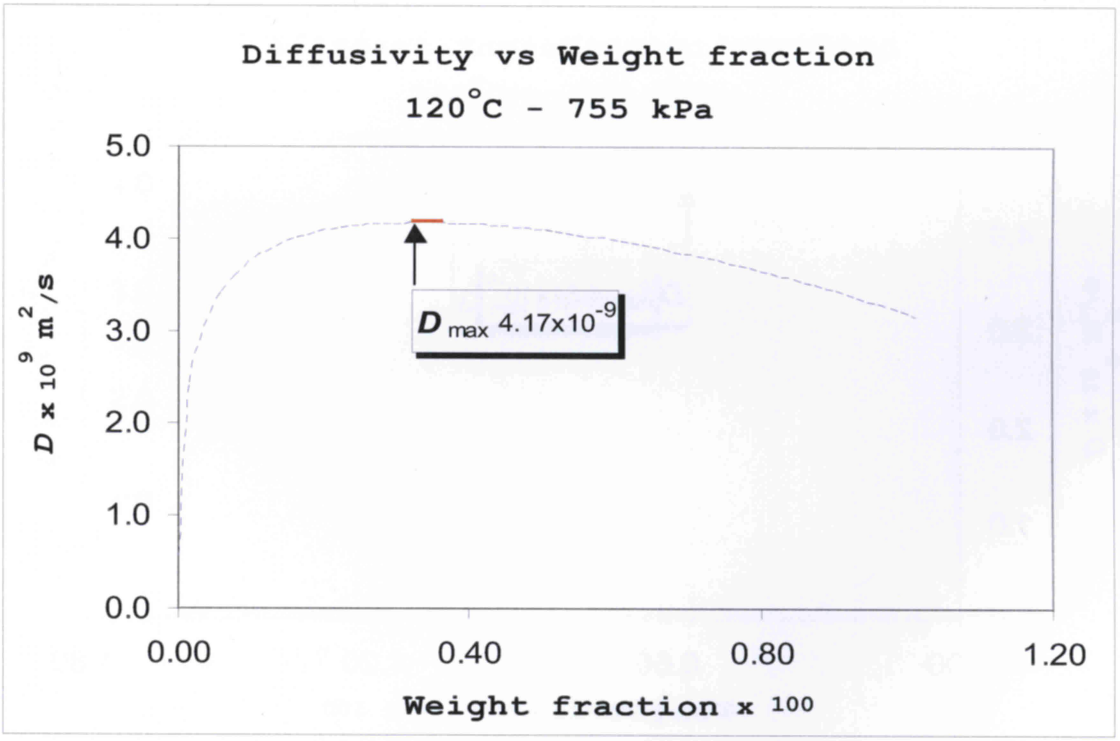

Figure 5. 5: Concentration dependent diffusivity plots D vs ω

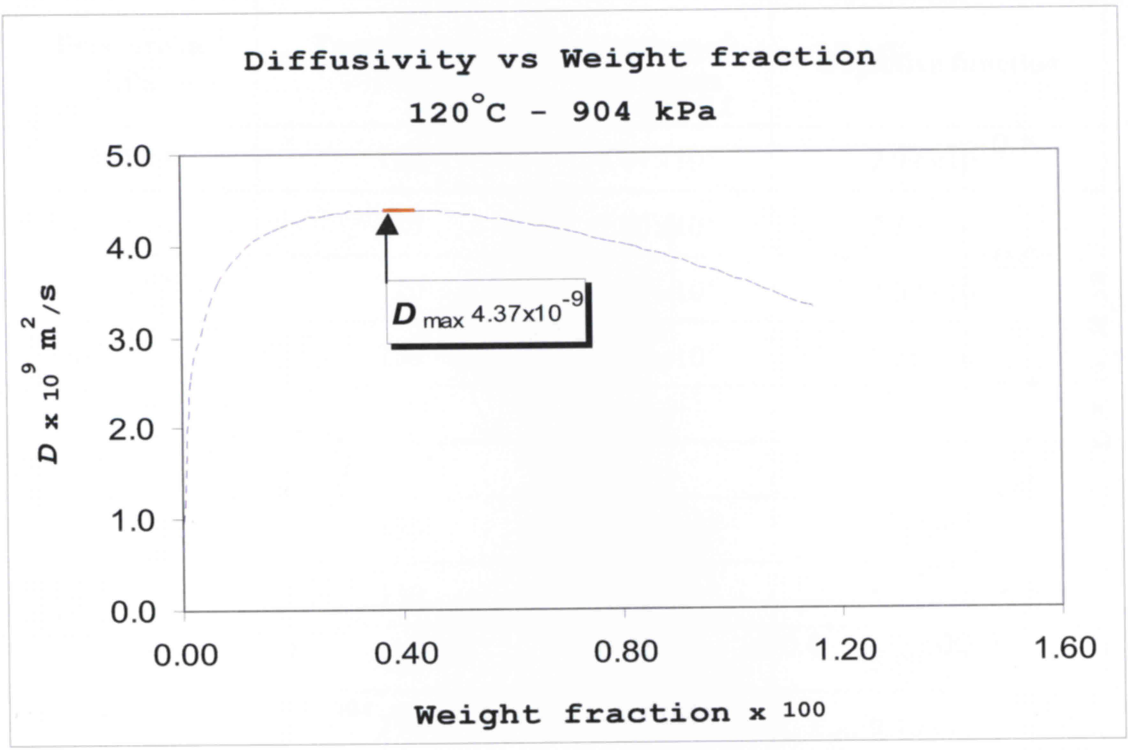

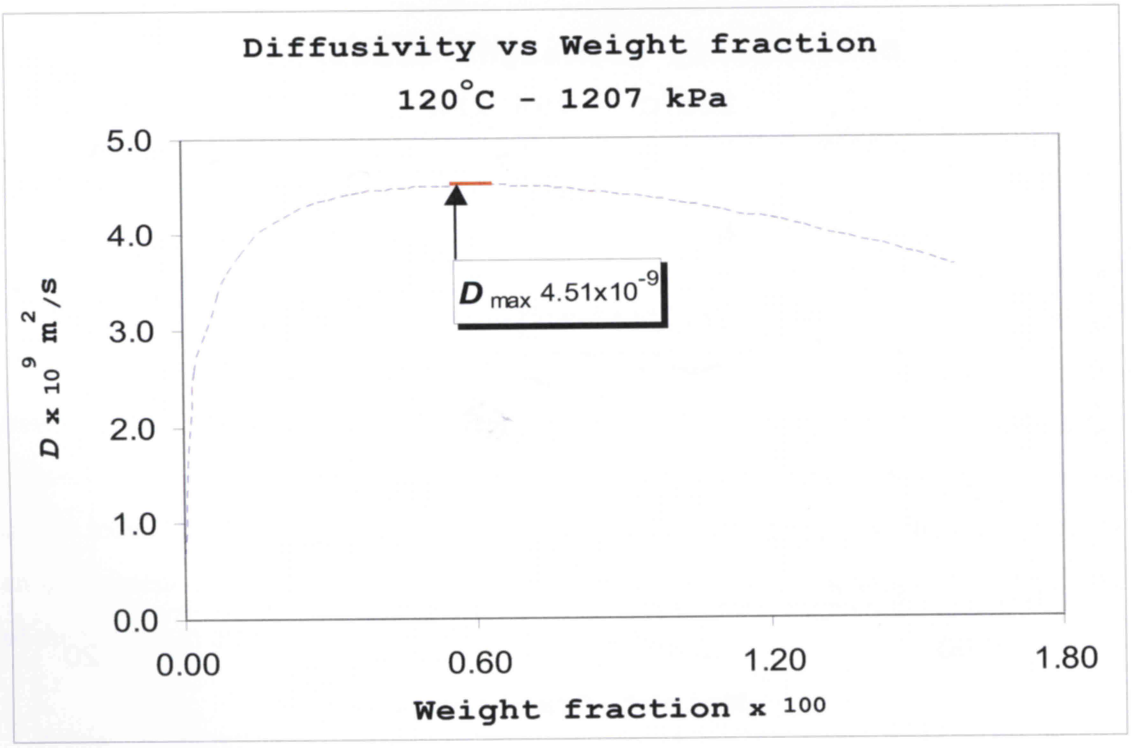

Figure 5. 6: Concentration dependent diffusivity plots D vs ω

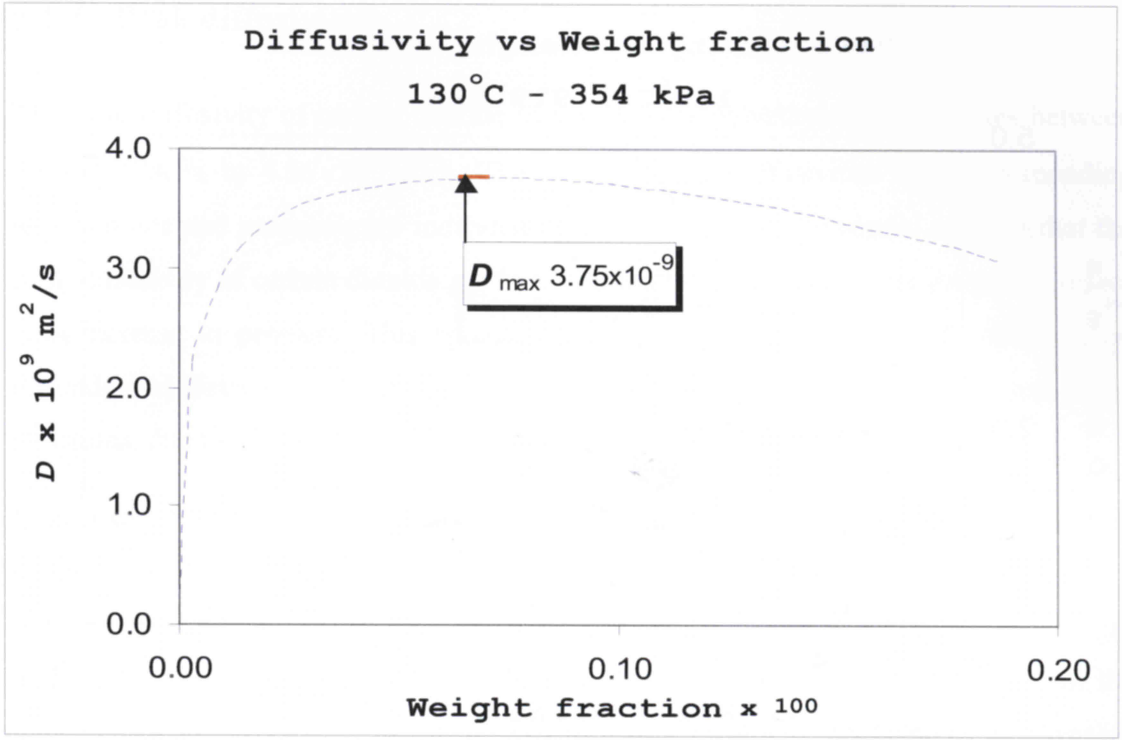

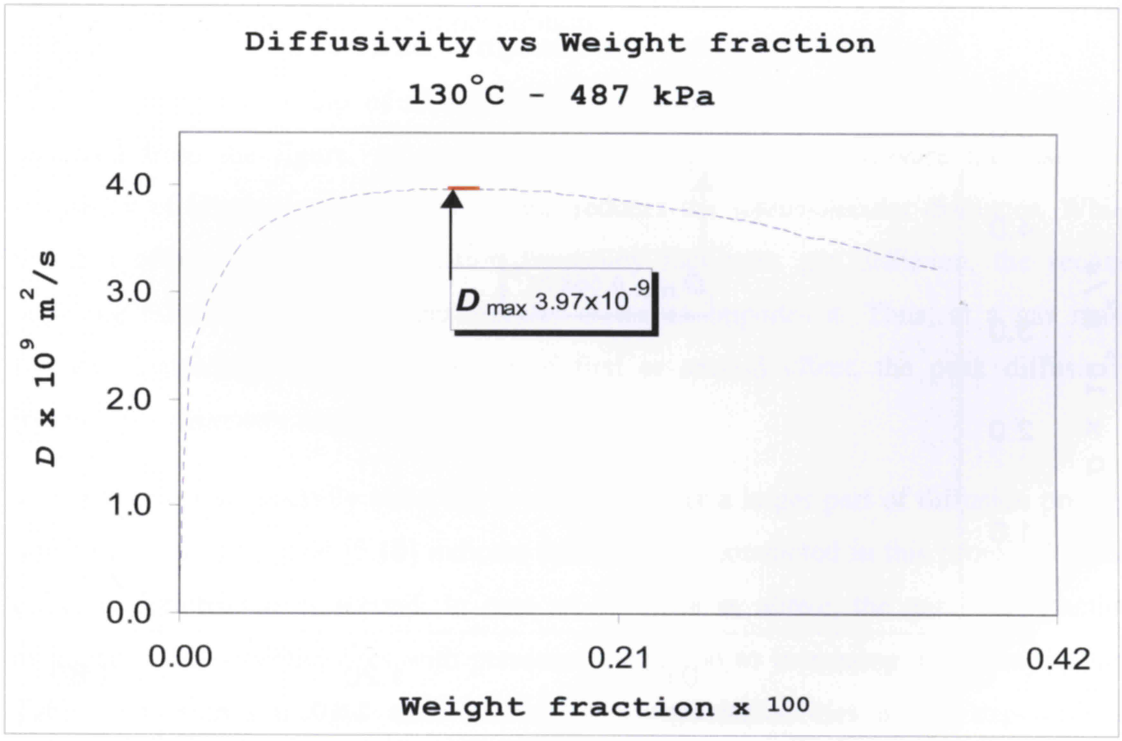

Figure 5. 7: Concentration dependent diffusivity plots D vs ω

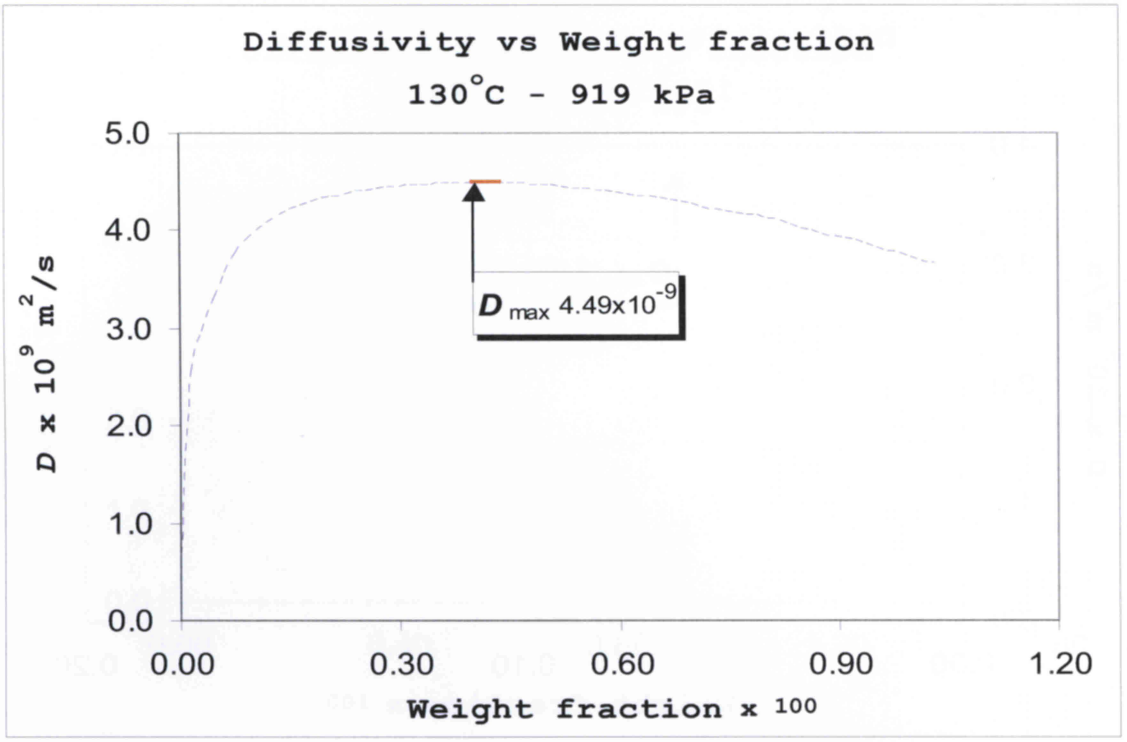

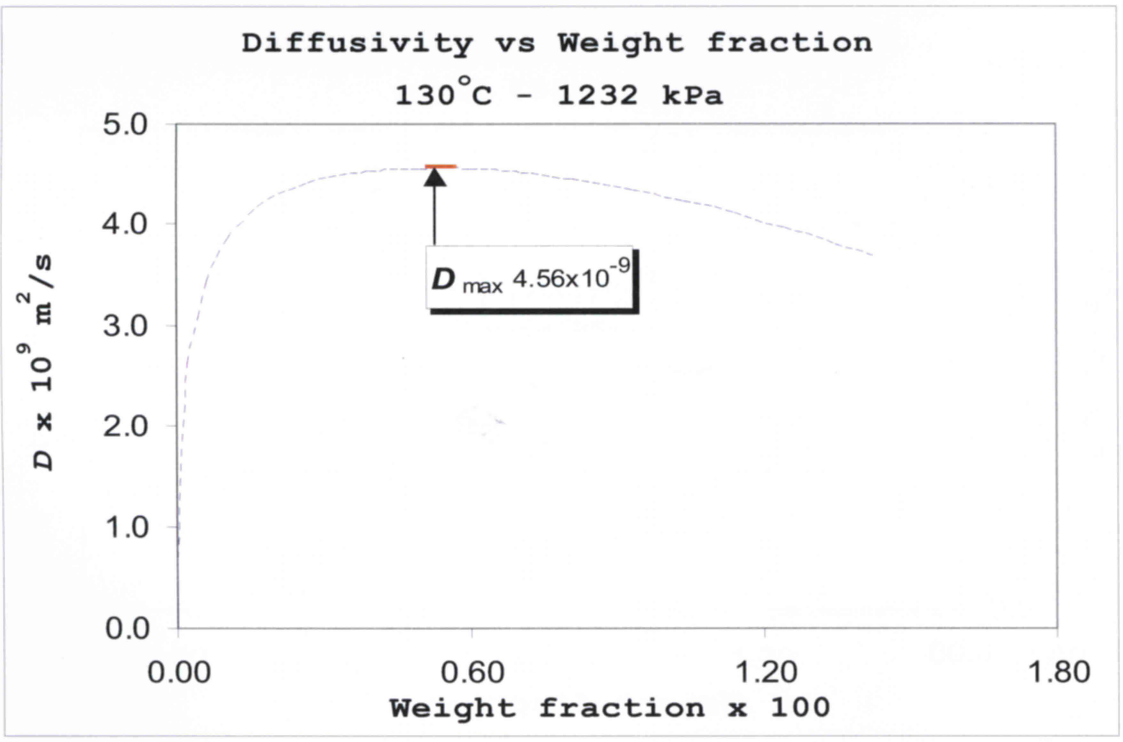

Figure 5. 8: Concentration dependent diffusivity plots D vs ω

5.1.3 Peak diffusivities

The peak diffusivity of carbon dioxide in low-density polyethylene melt varies between $3.04\times10^{-9}\,m^2/s$ to $4.56\times10^{-9}\,m^2/s$. The results of peak diffusivities with corresponding temperatures and pressures are indicated in the Table (5.2). The results indicate that the peak diffusivity of carbon dioxide gas in LDPE melt at a particular temperature increases with increase in pressure. This agrees with the established behavior of concentration dependent diffusivity and can be attributed to increase in the number of molecular collisions, due to increase in concentration, thus aiding diffusion.

It is also observed from the Table that peak diffusivity increases with increase in temperature. This can be attributed to the decrease in viscosity of the polymer, which reduces resistance to motion of molecules and also increase in kinetic energy of gas molecules. The Table (5.2) also indicates that for this LDPE sample and with in the temperature and pressure range of the experiment, peak diffusivity behavior is a weaker function of temperature than the concentration.

However, the relationship of diffusivity with pressure is not as straightforward as is observed from the figure. At a given gas fraction, a higher pressure increases the frequency of intermolecular collisions, but reduces the intermolecular distances. While the first effect of increased collision frequency facilitates gas diffusion, the second opposing effect of reduced intermolecular distances impedes it. Thus, at a gas mass fraction, depending on the dominance of first or second effect, the peak diffusivity increases or decreases respectively with pressure.

The first effect is generally observed to dominate over a larger part of diffusion process interval. Figure [5.9] and [5.10] indicate that for trials conducted in this project the first effect is dominant over second. In case of diffusion as above, the gas mass fraction averaged diffusivity increases with pressure in addition to increasing with temperature. Table (5.3) shows the gas mass fraction averaged diffusivities at the experimental conditions.

Pressure (kPa)	Peak D x $10^9 m^2/s$ 120°C	Weight fraction 120°C	Peak D x $10^9 m^2/s$ 130°C	Weight fraction 130°C	Reported D x$10^9 m^2/s$ 150°C	Weight fraction 150°C
352	3.402	0.00202	3.757	0.00186	-	-
487	-	-	3.976	0.00366	-	-
755	4.172	0.0103	-	-	-	-
904	4.379	0.011	-	-	-	-
919	-	-	4.494	0.01033	-	-
1207	4.514	0.0158	-	-	-	-
1232	-	-	4.560	0.01423	-	-
655*	-	-	-	-	4.4*	0.005*
1565*	-	-	-	-	3.9*	0.011*
2247*	-	-	-	-	-	0.015*
2999*	**-**	**-**	**-**	**-**	**4.6***	**0.020***
3364*	**-**	**-**	**-**	**-**	**4.4***	**0.023***

Table 5. 2: Experimental results for diffusivity and solubility of CO_2 gas in LDPE.
*** The constant diffusivity values from published data regarding similar polymer melt at 150°C.[26]**
The values in bold indicate the published data[26] obtained by more accurate dual chamber method.

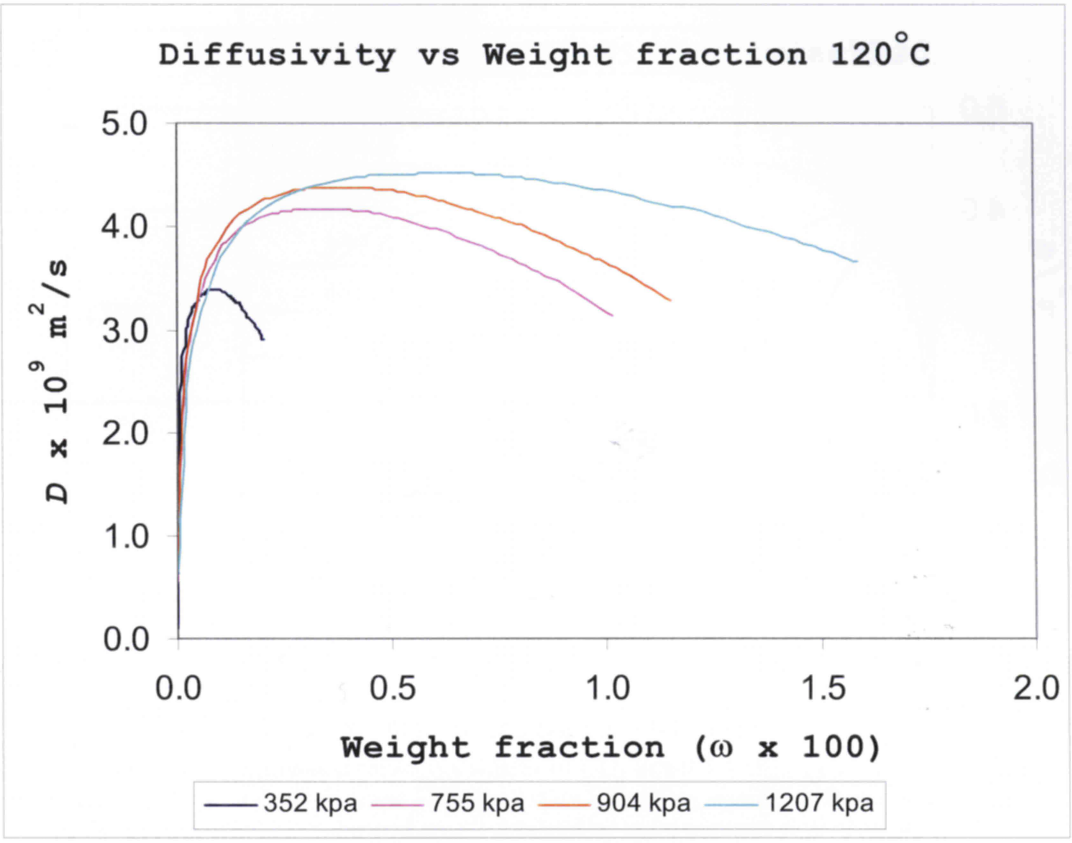

Figure 5. 9: Diffusivity curves at 120°C and different pressures.

Above plots indicate that peak diffusivities increase with increase in pressure.

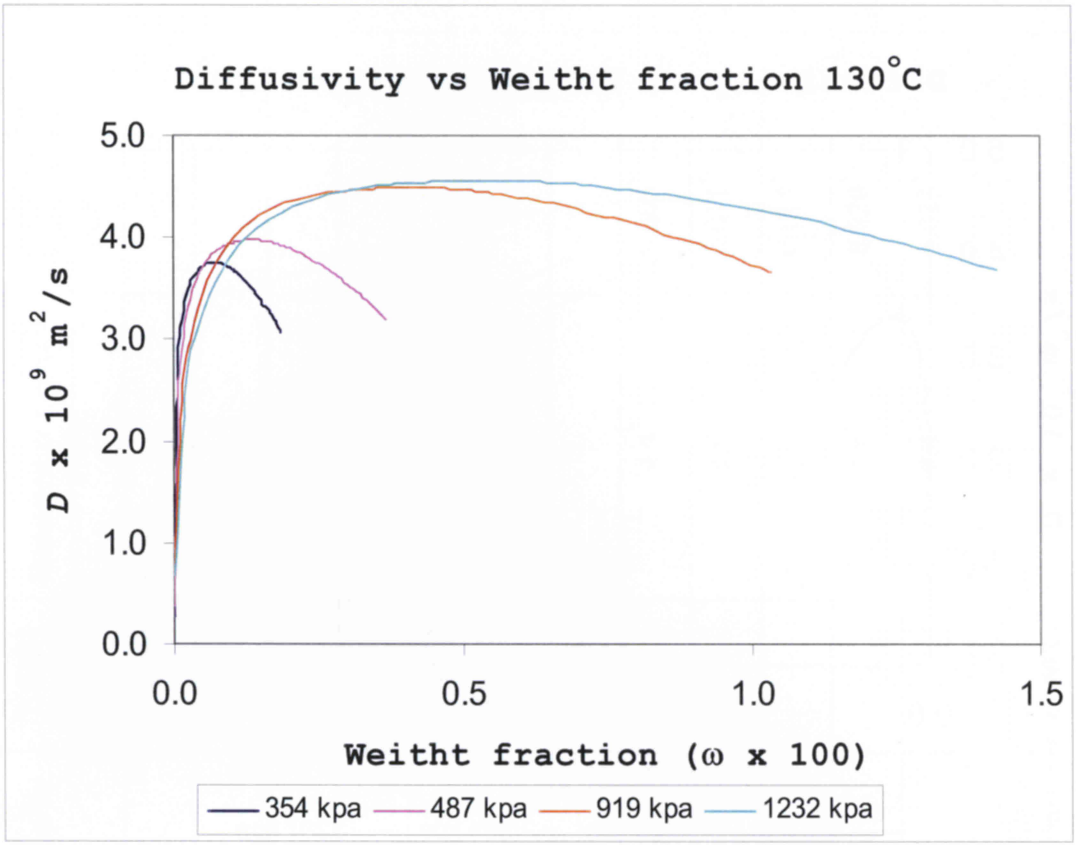

Figure 5. 10: Diffusivity curves at 130°C and different pressures.

Above plot of diffusivity curves at 130°C and different pressures indicate that peak diffusivities increase with increase in pressure.

Temperature (°C)	Pressure (kPa)	$D_{avg} \times 10^9$ (m^2/s)
120	352.0	3.15
	755.4	3.78
	904.3	3.97
	1207.2	4.15
130	354.0	3.46
	486.9	3.65
	919.5	4.14
	1232.4	4.20
150*	655*	4.4*
	1565*	3.9*
	2247*	-
	2999*	**4.6***
	3364*	**4.4***

Table 5. 3: Gas mass fraction-averaged diffusivity of CO_2 in the LDPE
*** The constant diffusivity values from published data regarding similar polymer melt at 150°C.[26]**
The values in bold indicate the published data[26] obtained by more accurate dual chamber method.

To figure out the relative dominance of pressure, temperature and concentration on diffusivity function is a complicated, multi-facet task. The response of diffusivity function to each of these factors is interdependent on others as well as on the changing response of morphology and compressibility of the polymer to its temperature, pressure and concentration.

5.1.4 Solubility

As observed in Figure [5.11], the maximum solubility of carbon dioxide in low-density polyethylene melt sample at a particular temperature increases with increase in pressure and decreases with increase in temperature at a particular pressure, which is in trend with related published literature.[26]

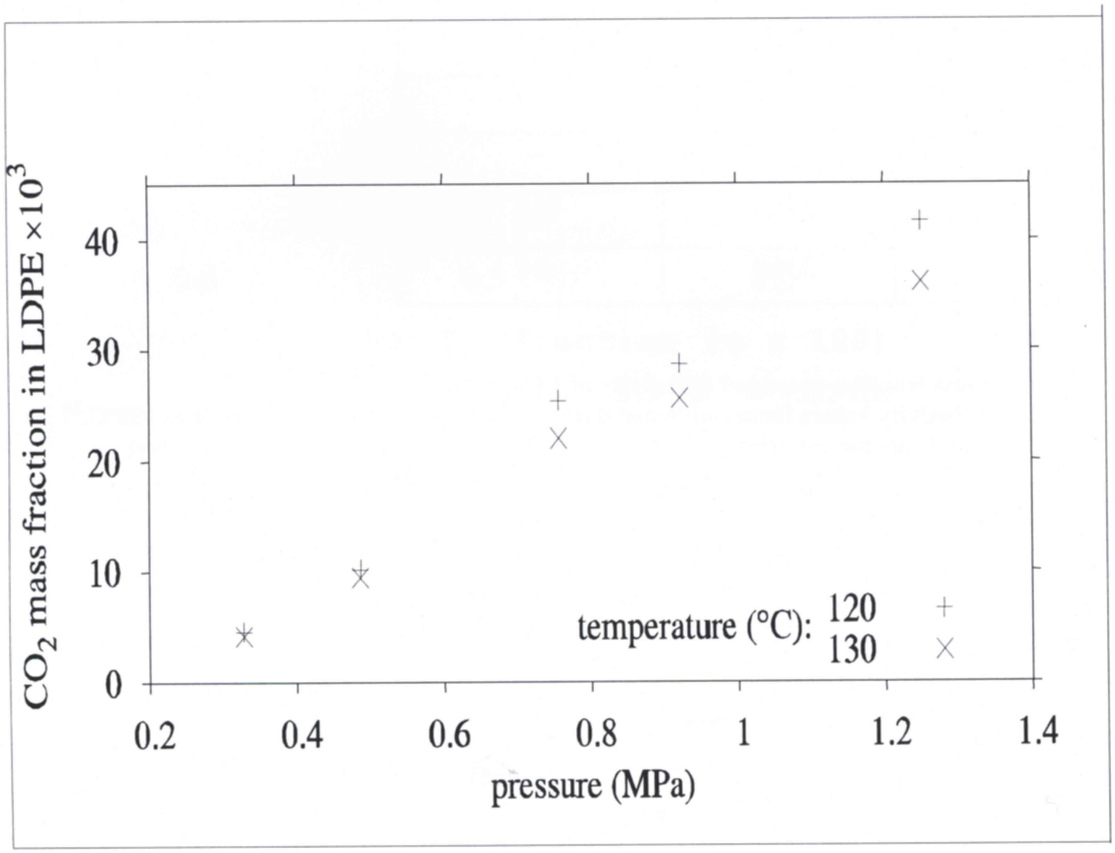

Figure 5. 11: The saturation mass fraction of carbon dioxide in the LDPE under the experimental conditions

5.1.5 Sensitivity

Though solution of the model through application of optimality criterion yield results and observations, which are in line with the published data, the model is supported by certain discreet parameters and data which characterize the polymer sample as well as the pressure decay system. The solution was analyzed and plotted for sensitivity to system volume and the sample density.

Sensitivity to gas volume change: As indicated in Figure [5.12] and [5.13], sensitivity analysis was carried out to determine the effect of deviation in the gas saturation mass fraction on diffusivity. It compares base value of gas diffusivity at highest and lowest pressures at 120°C and 130°C to those corresponding to ±2% variations in the gas phase volume. These variations conservatively embody the maximum possible error in the saturation gas mass fraction in the polymer. As observed from the figure, the three graphs overlap. In fact, the average of the absolute changes in the diffusivity is less than 0.07%.

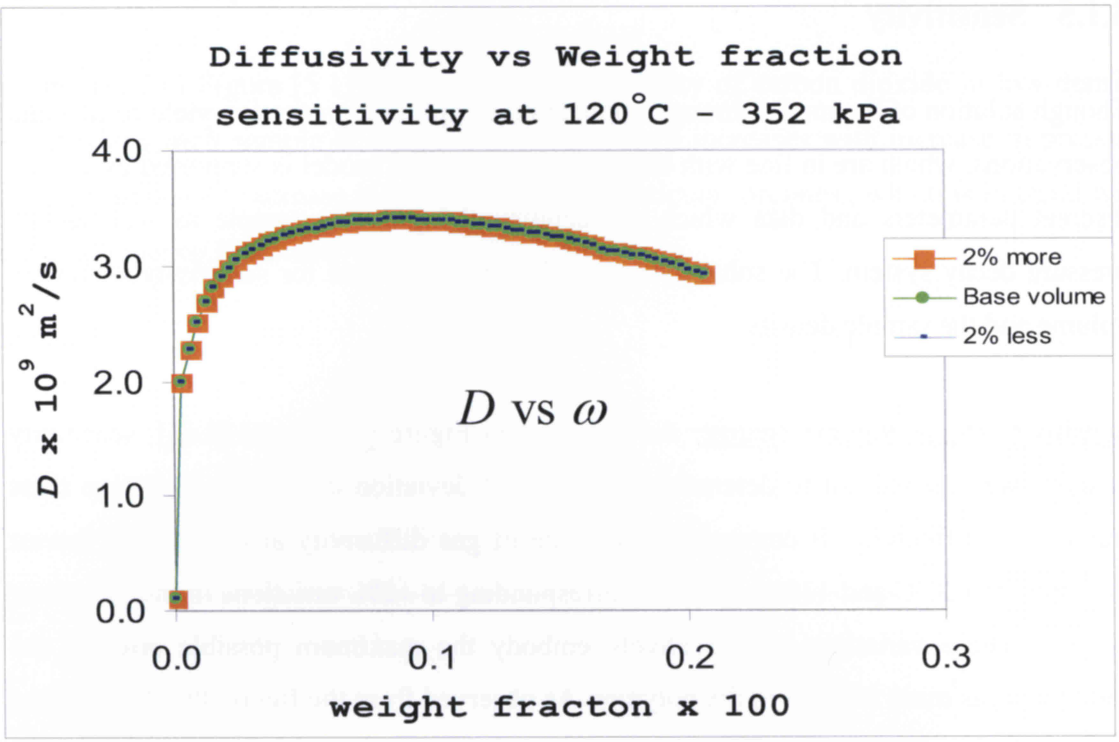

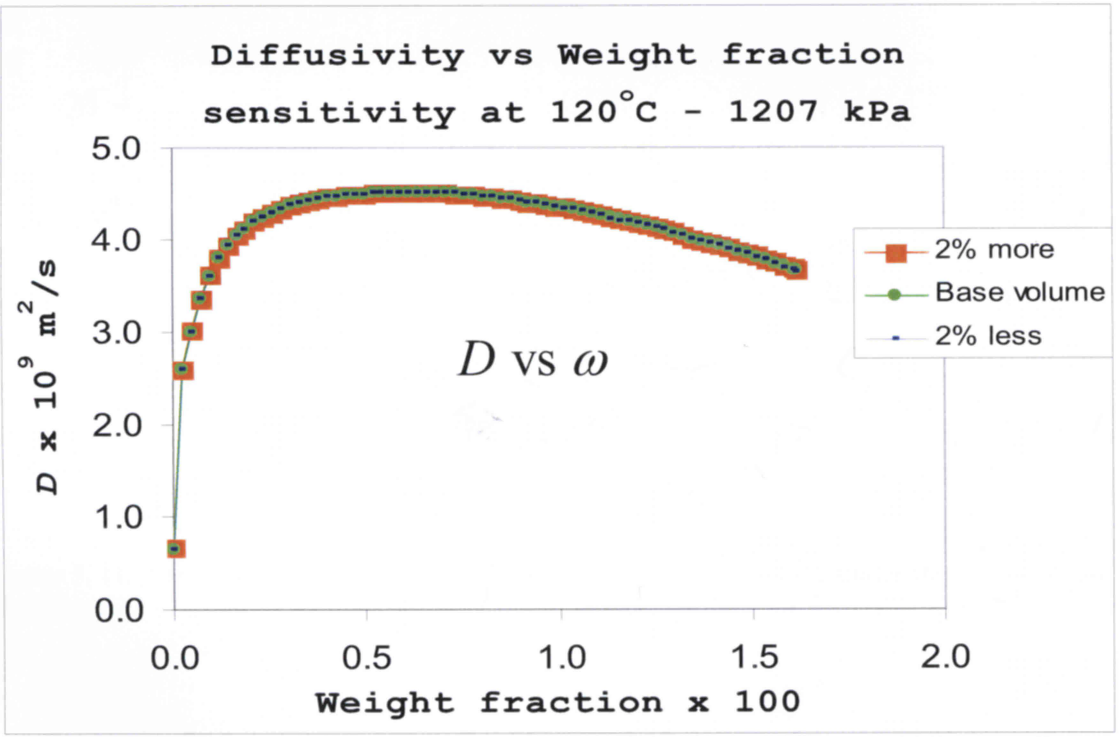

Figure 5. 12: Sensitivity of the diffusivity functional to gas volume at 120°C

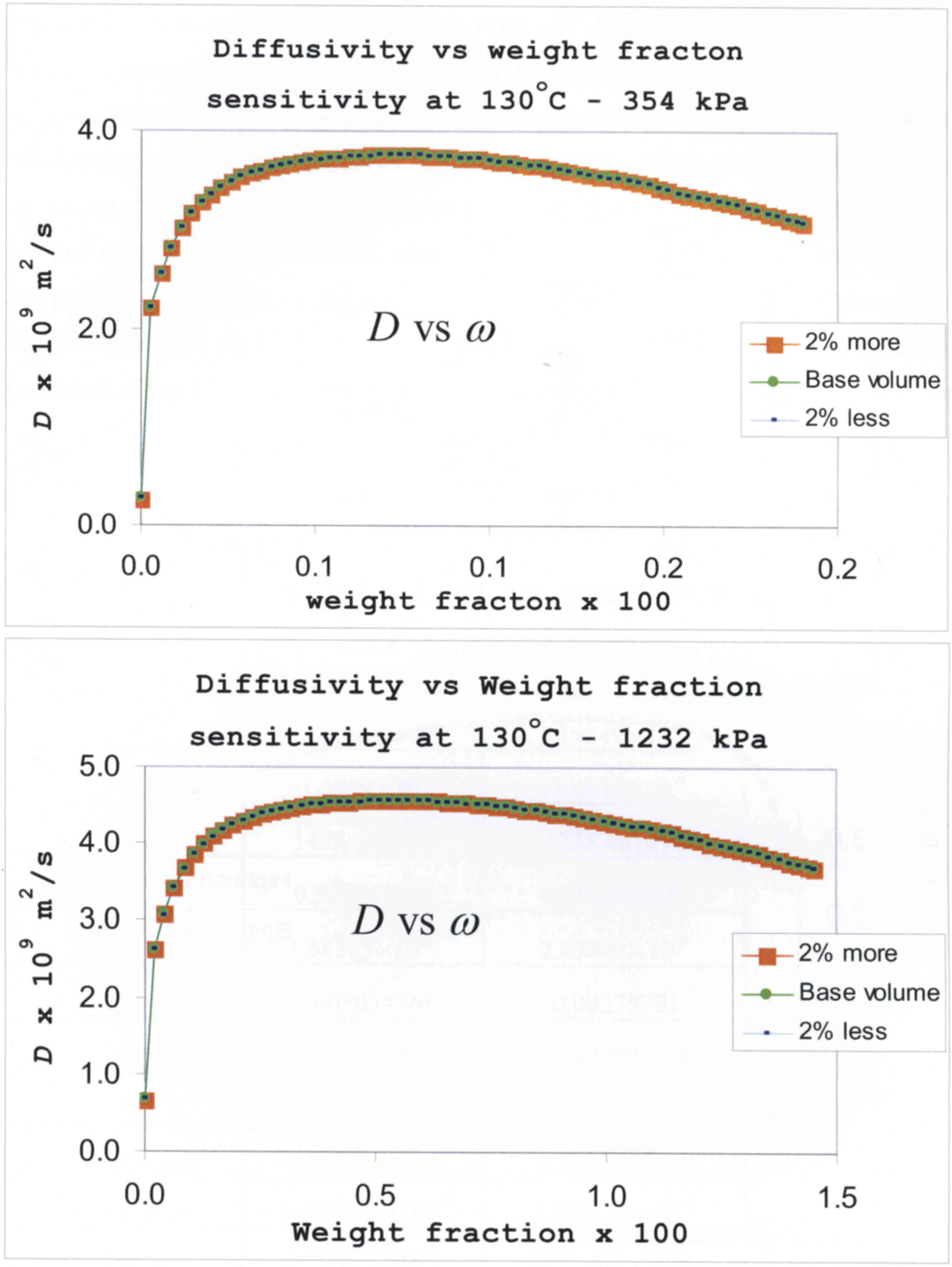

Figure 5. 13: Sensitivity of the diffusivity functional to gas volume at 130°C

Sensitivity to sample volume change: Any changes less than 10 microns occurring in the sample depth would go undetected. This error caused due to limitation of the experiment would affect the response of the model. In order to know the sensitivity to such a limitation following simulation exercise was carried out: it was assumed that diffusion of carbon dioxide into the sample would increase the volume of the sample resulting into swell of the sample in z direction by 10 microns. The change in depth would go unnoticed and also affect the density of the sample. Above change in volume and the corresponding change in density of the sample was used to calculate the diffusivity functional from the model. These results for 1232 kPa at 130°C were compared with the base case at the same pressure and temperature. Response of the model to the simulated change and its comparison with the base case is shown in Figure [5.14].

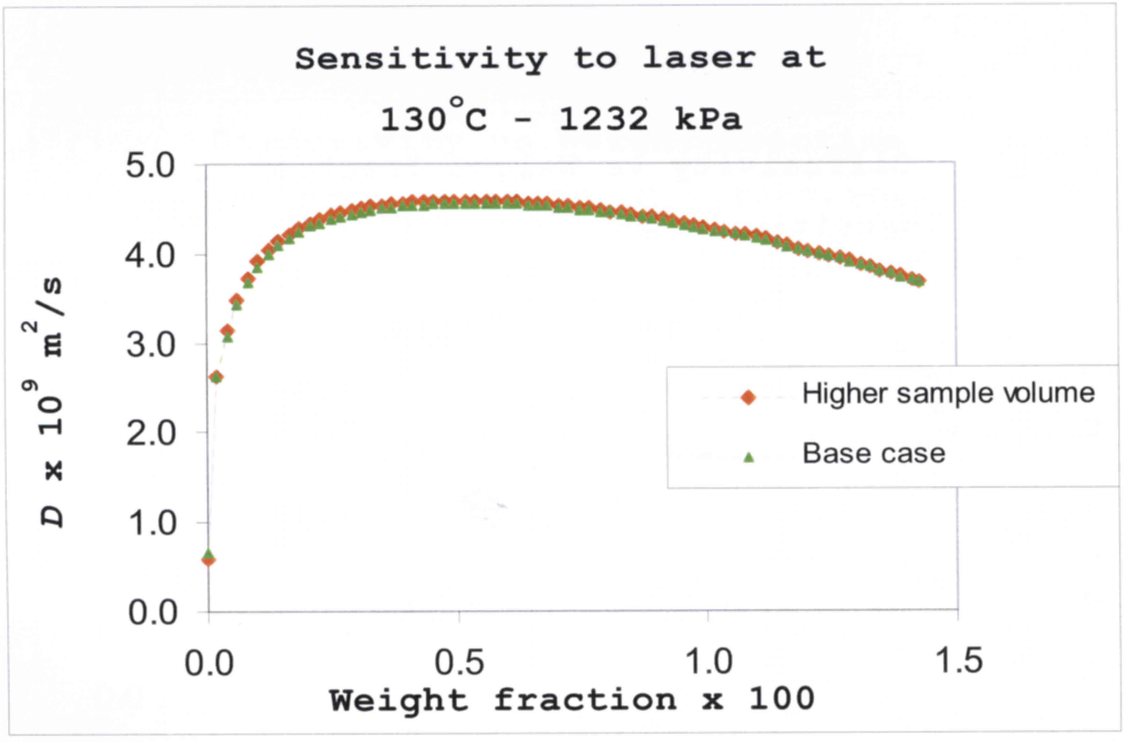

Figure 5. 14: Sensitivity to laser limitations.

Above plot shows the effect of probable changes beyond the least count of the laser equipment on the diffusivity output

5.2 Mathematical correlations for diffusivity

The diffusivity versus gas mass fraction data obtained in this work were mathematically correlated to obtain the diffusivity as a function of gas mass fraction and pressure at a given temperature. To that end, TCD3d™ was utilized to find the best fitting diffusivity in m^2/s as a function of pressure (P in kPa) and ω. That function is as follows:

$$D(P,\omega) = A_1 + A_2\,\text{lognorm}(A_3, A_4, P) + A_5\,\text{lognorm}(A_6, A_7, \omega) + A_8\,\text{lognorm}(A_3, A_4, P)\,\text{lognorm}(A_6, A_7, \omega) \tag{5.1}$$

In the above correlation, the log-normal function is defined as

$$\text{lognorm}(a_1, a_2, x) = \exp\left\{-0.5\left[\frac{\ln(x/a_1)}{a_2}\right]^2\right\} \tag{5.2}$$

Parameter	120°C	130°C
A_1	1.65397×10^{-9}	1.19849×10^{-9}
A_2	-1.6609×10^{-9}	-1.0842×10^{-9}
A_3	1498.647155	1223.481874
A_4	0.598411078	0.503400309
A_5	1.68385×10^{-9}	2.45502×10^{-9}
A_6	0.003034766	0.00273781
A_7	2.655924519	3.468470719
A_8	2.95041×10^{-9}	1.87555×10^{-9}
r^2 coefficient	0.8725247765	0.8223087606
fit std. error	2.329589×10^{-10}	2.622134×10^{-10}
F-statistic	265.96399644	178.49852205

Table 5. 4: Parameters for the diffusivity correlation Equation (5.2) at a given temperature

5.3 Conclusion

A methodology was developed to experimentally determine the concentration-dependent diffusivity of a gas in a non-volatile phase such as polymer. Pressure decay with solute–medium interface tracking capability with simultaneous measurement of swelling in polymer medium, was used for date generation. Using the methodology, the diffusivity of carbon dioxide was determined as a function of its concentration in LDPE at 120°C and 130°C for four different pressures in the range 352 to 1232 kPa. The diffusivity functions were found to be strongly unimodal with concentration dependent variations up to 96%. The diffusivities values are of the order 10^{-9} m^2/s. A confidence of ±1% in the diffusivity values is indicated by the sensitivity analysis carried out with respect to the maximum deviation in the gas phase volume or experimentally determined gas solubility. Based on the diffusivity data produced in this work, concentration-averaged diffusivity values and mathematical correlations were generated.

5.4 Future work and recommendations

Above developed methodology can be further improved on two grounds as follows:

Materials and technology:

a. The pressure decay cell can be redesigned with stronger and lighter materials as titanium. More strength would expand the experimental pressure range up to approximately 5000 psig and lighter weight would facilitate simultaneously gravimetric confirmation of gas uptake rate.
b. Better laser beams available now are capable of improving the sensitivity and accuracy of the apparatus.

Applications:

The improved apparatus can be used for finding concentration dependent diffusion curves for larger solute molecules at higher pressures.

1. Optimal sample size trials for generated diffusivity functional.
2. Concentration dependent diffusivity curves for polymer solvent systems with larger solute molecules and at higher pressures.
3. Study the compatibility of dimensionless parameters in objective function.
4. Comparative study of concentration dependent diffusivity and constant diffusivity with respect to sorption rate curves.
5. Study the concentration distance curves for concentration dependent diffusivity functional.

6 References

1. Brockmeier, N.F. and Rogan, J.B. Simulation of continuous Polymerization in a Backmix reactor using some batch kinetic data, Continuous Polymerization Reactors, Bouton, T.C. and Chappeler, D.C. eds., AIChE Sym. *American Institute of Chem. Engrs.,* New York **1976** Series 160, 72

2. Biesenberger, J.A., *Polymer Engr. and Sci.*, **1980**, 20, 1015

3. Biesenberger, J.A. Devolatilization of Polymers Fundamentals of Equipment – Applications *New York, Hanser,* **1983**

4. Krishna, R.; Wesselingh. J.A. The Maxwell – Stefan Approach to mass transfer *Chem. Eng. Sci.* **1997**, 52(6), 861-911

5. Felder, R.M.; Huvard, G.S.Methods of Experimental Phusics, Vol 16C, eds. Marton, L. and Marton, C. *Academic Press, New York*, **1980**, 315-77

6. Crank, J. and Park, G.S. eds. Diffusion in Polymers, *Academic Press, New York*, **1968**, 20-25

7. Yasuda, H. and Stannett, V. Special Problems and Methods in the Study of Water Vapor Transport in Polymers, *J. Macromol. Sci-Phys,* **1969**, B3(4), 589-610

8. Felder, R.M.; and Huvard, G.S. Methods of Experimental Physics, Vol 16C, eds. L. Marton and C. Marton, *Academic Press, New York*, **1980**, 362-63

9. Corea; C.R. and Klien, A. Measurement of Permeability, Diffusion and Solubility Coefficients a Testing Method *Polymer Testing,* **1990,** 9, 271-277

10. Koros, W.J. and Paul, D.R. Transient and Steady-State Permeation in Poly(ethylene Terephthalate) Above and Below the Glass Transition *J. Polym. Sci.: Polym. Phys. Ed.,* **1978**, 16. 2171-2187

11. Michaels, A.S.; Vieth, W.R. and Barrie, J.A. Solution of Gases in Polyethylene Terephthalate *J. Appl. Phys.,* **1963**, 34(1), 1-12

12. Koros, W.J.; Paul, D.R. and Rocha, A.A. Carbon Dioxide Sorption and Transport in Polycarbonate, *J. Polym. Sci.:Polym, Phys. Ed.,* **1976**, 14, 687-702

13. Michaels, A.S.; Vieth, W.R. and Bixler, H.J. Gas Permeability of Highly Oriented Dibuty1 Maleate-Ethylene Copolymer Films, *J. Appl. Polym. Sci.,* **1964**, 8, 2735-2750

14. Felder, R.M. and Huvard, G.S. Methods of Experimental Physics, Vol. 16C, eds. Marton, L. and Marton, C. *Academic Press, New York*, **1980,** 364

15. Felder, R.M. and Huvard, G.S. Methods of Experimental Physics, Vol. 16C, eds. Marton, L. and Marton, C. *Academic Press, New York*, **1980**, 339

16. Kalachandra, S. and Turner, D.T. Water Sorption of Poly(methyl methacrylate): 3. Effects of Plasticizer, *Polymer,* **1987,** 28, 1749

17. Urdahl, K.G. and Peppas, N.A. Anomalous Penetrant Transport in Glassy Polymers V. Cyclohexane Transport in Polystyrene, *J. Appl. Polym. Sci.,* **1987,** 33, 2669-2687

18. Aminabhavi, T.M.; Thomas, R.W. and Cassidy, P.E. Predicting Water Diffusivity in Elastomers, *Polym. Eng. Sci.,* **1984,** 24(18), 1417-1420

19. McBain, J.W. and Bakr, A.M. A New Sorption Balance, *J. Am.Chem. Soc.,* **1926,** 48, 690-695

20. Rosan, B. A. Recording Sorption Kinetics Apparatus, *J. Polym. Sci.,* **1959,** 35, 335-342

21. Palamara, J.E.; Davis, P.K.; Uthaiporn Suriyapraphadilok,U.; Danner, R.P.; Duda, J.L., Kitzhoffer, R.J. and Zielinski J.M. Static sorption technique for vapour solubility measurements *Ind. Eng. Chem. Res.* **2003,** 42, 1557-1562

22. Newitt,.D.M.; Weale,K.E.; Solution and diffusion of gases in polystyrene at high pressures *J. Chem.Soc.(London)* **1948** IX, 1541

23. Lundberg, J.L.; Wilk, M.B.; Huyett, M.J. Sorption studies using automation and computations. *Ind. Eng. Chem. Fundam* **1963**, 2, 37

24. Koros, W.J.; Paul, D.R. Design considerations for measurment of gas sorption in polymers by pressure decay. *J. Polymer Science B: Polymer Physics*. **1976**, 14, 1903-1907

25. Cussler, E.L. Diffusion Mass Transfer in Fluid Systems, Second Edition, *Cambridge University Press,* **1999**

26. Dawis, P.K.; Lundy, G.D.; Palamora, J.E.; Duda, J.L.; and Danner, R.P. New pressure decay techniques to study gas sorption and diffusion in polymers at elected pressures *Ind. Eng. Chem. Res.* **2004**, 43, 1537-1542

27. Upreti, S.R.; and Mehrotra, A.K. Experimental measurement of gas diffusivity in bitumen *Ind. Eng. Chem. Res*. **2000**, 39, 1080-1087

28. The fifth-order adaptive step method of Runge-Kutta-Fehlberg with Cash-Karp parameters (Press et al., 2002)

29. Press, W. H.; Teukolsky, S. A.; Vetterling, W.T.; Flannery, B.P. Numerical Recipes in C: The Art of Scientific Computing, 2nd ed.; *Cambridge University Press*: New York, **1995**

Appendix A

Calculation of $m_{gp,e}(t)$ and ω_{sat}

Specific molar volume of CO_2 at experimental pressure is obtained from the PVT data plots. As shown in Figure [A1] experimental pressures are plotted against PVT data to obtain $\bar{V}$ at experimental pressures.

The constant pressure, $\bar{V}$ versus T plots are obtained at experimental pressures, by the above procedure. As shown in Figure [A2] the experimental temperatures are plotted on the above $\bar{V}$ versus T plots to get $\bar{V}$ at experimental temperature and pressure. The moles of CO_2 gas present in the pressure decay chamber at experimental temperature and pressure is given by

$$M_g(t) = \frac{V_g(t)}{\bar{V}} \tag{A1}$$

where $M_g(t)$ is the moles of CO_2 gas present in pressure decay volume; $V_g(t)$ is the pressure decay volume.

Similarly $M_g(0)$; moles of gas present in pressure decay volume at time $t = 0$ can be obtained by above plots.

$m_{gp,e}(t)$; mass of gas absorbed by polymer at time t is given by

$m_{gp,e}(t) = \left[M_g(0) - M_g(t) \right] \times$ molecular weight of CO_2

The value of $m_{gp,e}(t)$ at final pressure corresponding to the end of an experiment yields saturation mass fraction of gas, i.e. $\omega_{sat}[P(t)]$

The saturated gas mass of CO_2 gas in polymer sample can also be obtained by calculating $\bar{V}$ at saturation pressure P_{sat} by above procedure. As weight of polymer is known, saturated gas mass fraction of CO_2 ω_{sat} can be calculated.

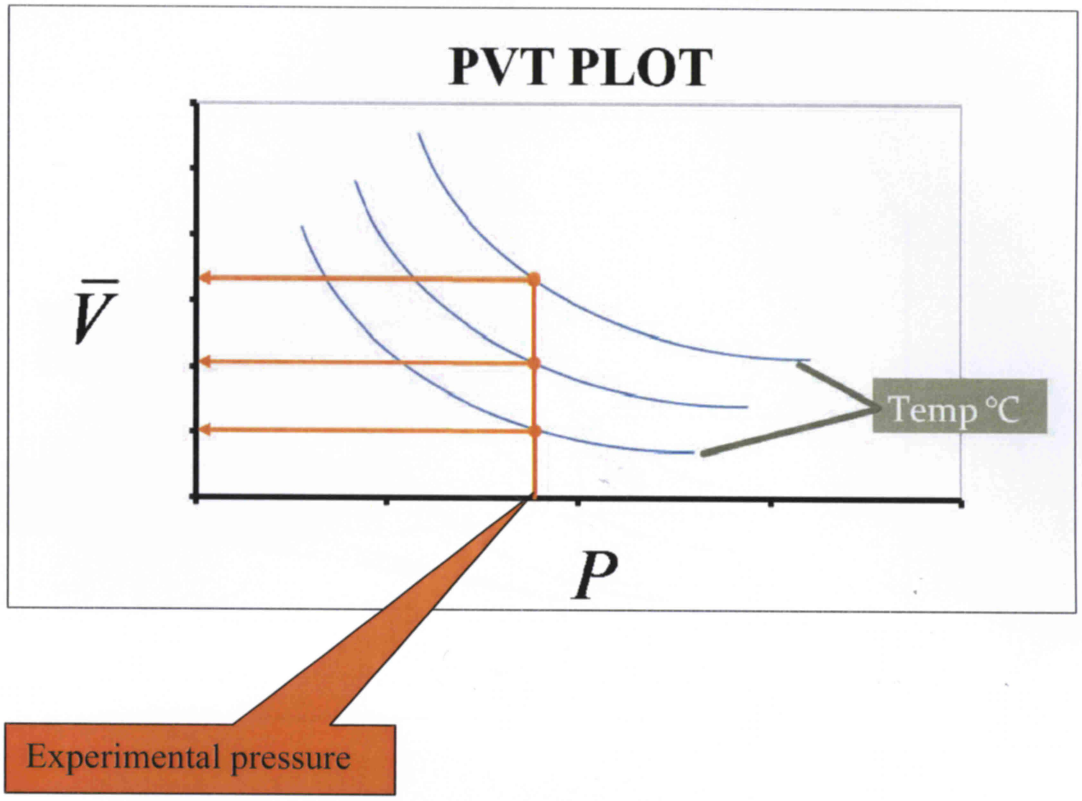

Figure A 1: $\bar{V}$ at experimental pressure from PVT data

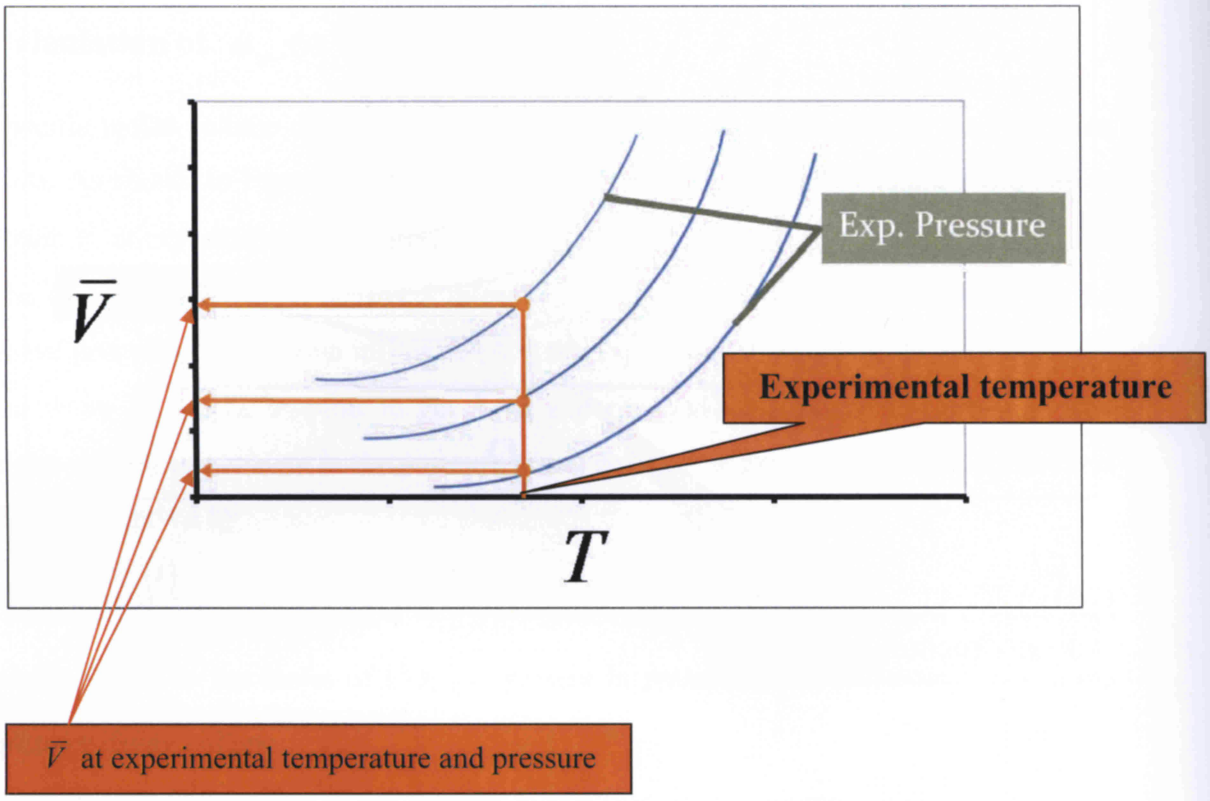

Figure A 2: $\bar{V}$ at experimental temperature and pressure